EMBRY-RIDDLE
Aeronautical University
SCHOLARLY COMMONS

PhD Dissertations and Master's Theses

12-2021

Optimal Sizing and Control of Hybrid Rocket Vehicles

SRIJA RYAKAM
ryakams@my.erau.edu

Follow this and additional works at: https://commons.erau.edu/edt

 Part of the Navigation, Guidance, Control and Dynamics Commons, Other Aerospace Engineering Commons, Propulsion and Power Commons, and the Space Vehicles Commons

Scholarly Commons Citation

RYAKAM, SRIJA, "Optimal Sizing and Control of Hybrid Rocket Vehicles" (2021). *PhD Dissertations and Master's Theses*. 629.
https://commons.erau.edu/edt/629

This Dissertation - Open Access is brought to you for free and open access by Scholarly Commons. It has been accepted for inclusion in PhD Dissertations and Master's Theses by an authorized administrator of Scholarly Commons. For more information, please contact commons@erau.edu.

OPTIMAL SIZING AND CONTROL OF HYBRID ROCKET VEHICLES

By

SRIJA RYAKAM

A Dissertation Submitted to the Faculty of Embry-Riddle Aeronautical University

In Partial Fulfillment of the Requirements for the Degree of

Doctor of Philosophy in Aerospace Engineering

December 2021

Embry-Riddle Aeronautical University

Daytona Beach, Florida

OPTIMAL SIZING AND CONTROL OF HYBRID ROCKET VEHICLES

By

SRIJA RYAKAM

This Dissertation was prepared under the direction of the candidate's Dissertation Advisor, Dr.Yechiel Crispin, Department of Aerospace Engineering, and has been approved by the members of the Dissertation Committee. It was submitted to the Office of the Senior Vice President for Academic Affairs and Provost, and was accepted in the partial fulfillment of the requirements for the Degree of Philosophy in Aerospace Engineering.

DISSERTATION COMMITTEE

Chairman, Dr. Eric Perrell	Advisor, Dr. Yechiel Crispin
Member, Dr. Reda Mankbadi	Member, Dr. Mark Ricklick
Member, Dr. Richard Prazenica	Member, Dr. William MacKunis
Graduate Program Coordinator, Dr. Sirish Namilae	December 9, 2021 Date
Dean of the College of Engineering, Dr. James Gregory	December 9, 2021 Date
Senior Vice President for Academic Affairs and Provost, Dr. Lon Moeller	December 10, 2021 Date

ACKNOWLEDGEMENTS

It's a great pleasure to acknowledge my deepest gratitude to my advisor Dr. Yechiel Crispin for his constant guidance and motivation, without which this work would not have been possible. I would like to express my sincere thanks to committee chair Dr. Eric Perrell, and committee members Dr. Reda Mankbadi, Dr. Mark Ricklick, Dr. Richard Prazenica, and Dr. William MacKunis for reviewing my work and providing many valuable comments. I would like to extend my appreciation to all the faculty members of the Department of Aerospace Engineering for their support and encouragement. I also would like to take a moment here to thank my parents and family members for their constant love and unyielding support. I owe a debt of gratitude to my friends who supported me during my research work.

ABSTRACT

In the present work, a genetic algorithm is used to optimize a hybrid rocket engine in order to minimize the propellant required for a specific mission. In a hybrid rocket engine, the mass flow rate of the oxidizer can be throttled to enhance the performance of the rocket. First, an analysis of the internal ballistics and the ascent trajectory has been carried out for different mass flow rates of the oxidizer as a function of time, for a fixed amount of oxidizer, in order to study the effect of throttling. Two equivalent problems are considered: in the first problem the amount of propellant is fixed, and we are seeking the oxidizer mass flow rate as the function of time such as to maximize the altitude. In the second problem, we obtain the mass flow rate of the oxidizer as a function of time in order to minimize the propellant required to reach a specific altitude. A genetic algorithm is used to find the best mass flow rate of the oxidizer. The optimization is carried out for two different regression rate laws, one depending only on the oxidizer mass flux rate and the other one depending on the mass flux rate of the oxidizer and the fuel. The results obtained in both cases are similar and show that the mass flow rate of the oxidizer should be maximized up to about one-third of the burn time and then decreased gradually. Using this mass flow rate of the oxidizer, we obtain the best initial oxidizer to fuel ratio in order to perform an optimal sizing of the rocket.

TABLE OF CONTENTS

LIST OF FIGURES

Figure Page

Figure Page

LIST OF TABLES

NOMENCLATURE

A_p	Area of the port
a	Regression rate coefficient
D_{H0}	Initial hydraulic diameter
D_H	Hydraulic diameter
F	Thrust
G_{f0}	Initial fuel mass flux rate
G_{ox0}	Initial oxidizer mass flux rate
G_f	Fuel mass flux rate
G_{ox}	Oxidizer mass flux rate
g	Acceleration due to gravity
h	Altitude
h_m	Characteristic altitude
h_b	Altitude at burn out
L_p	Length of the port
M_0	Initial mass of the vehicle
M	Mass of the vehicle
m, n	Regression rate exponents
$\dot{m}_{f0}$	Initial fuel mass flow rate
$\dot{m}_{ox0}$	Initial oxidizer mass flow rate
$\dot{m}_{p0}$	Initial propellant mass flow rate
$\dot{m}_f$	Fuel mass flow rate
$\dot{m}_{ox}$	Oxidizer mass flow rate

$\dot{m}_p$	Propellant mass flow rate
N	Number of ports
OF_0	Initial oxidizer to fuel ratio
OF	Oxidizer to fuel ratio
P_p	Perimeter of the port
$\dot{r}_0$	Initial regression rate
$\dot{r}$	Regression rate
u_e	Exit velocity
v	Velocity
v_c	Characteristic velocity
v_b	Velocity at burn out
w	Fuel web thickness used
ρ_f	Fuel density
τ	Characteristic time

1. Introduction

The dynamic optimization or the optimal control problem deals with finding the time histories of the controls and the state variables for a dynamic system such that an objective function is optimized (Vinter, 2002). Modern optimal control methods are based on Pontryagin's maximum principle. These methods are an extension of the classical method of the calculus of the variations (Fox, 1987). Pontryagin's maximum principle provides the necessary conditions for optimality, which are first-order differential equations. This results in a two-point boundary value problem (TPBVP) for the state and the adjoint variables (Pontryagin, 1987). The TPBVPs are more difficult to solve than the initial value problems. To avoid solving the TPBVP, direct optimization methods have been developed (Crispin, 2007).

1.1. History

The Brachistochrone problem is the first minimum-time optimal control problem, proposed by John Bernoulli in the 17th Century (Ben-Asher, 2010). The problem is to find the shape of the wire to minimize the time required for a bead to descend along a frictionless wire due to gravity. Ever since, numerous ideas were developed to solve similar kinds of problems using the calculus of variations (Ross, 2015). The important developments are the derivation of Euler-Lagrange equations for obtaining optimal solutions, the Legendre condition for a weak minimizer and a Weierstrass condition for a strong minimizer, and the Jacobi condition for non-conjugate points (Ben-Asher, 2010).

Lippisch (1946), a German aircraft designer, solved optimal control problems of atmospheric flight by applying the methods of the calculus of variations, but he did not obtain the right formulation of the Euler- Lagrange equations.

In 1949, M. Hestenes considered a minimum-time problem for aircraft climb performance. He applied the calculus of variations method. He formulated the maximum principle as a translation of the Weierstrass condition. Unfortunately, the original work was never published (Hestenes, 1950). Berkovitz presented Hestenes's work, indicating that it is more general than the maximum principle as it includes state-dependent control bounds (Berkovitz, 1961).

In 1953, Bushaw and his advisor S. Lefschetz at Princeton University considered time-optimal control problems outside of the calculus of variations. He considered a non-linear oscillator formulated by the intuition that the maximum available power yields the best results for the minimum-time problem. The optimal trajectories in the phase-plane are obtained to be canonical paths (Bushaw, 1953; Bushaw, 1958).

During the 1960's the maximum principle was the primary tool for solving optimal control problems. The main application was flight trajectory optimization. Kelly developed a generalized Legendre condition for singular arcs. But the Jacobi condition could not be generalized to singular cases (Kelly et al., 1967). Even though it was not successful for singular cases, employing the Jacobi condition was successful for regular cases of optimal control (Breakwell et al., 1963). This concept opened the way for closed-loop implementations of optimal control with the use of secondary extremals. It was used in, for example, the re-entry phase of the Apollo flights (Kelly, 1962; Breakwell et al.,1965).

The maximum principle transforms the optimal control problem into a TPBVP. In most cases, it is very difficult to obtain the solution for TPBVP. Therefore, many

numerical methods have been developed to overcome this problem. Many gradient-based methods were developed to solve discrete-time optimal control problems (Mayne, 1966).

Kelly proposed a method to provide an analytical approximation to the exact solution by employing singular perturbation in optimizing flight trajectories to facilitate the TPBVP solution process (Kelly, 1973).

Murray and Yakowitz (1984) developed Newton's Method and differential dynamic programming to solve discrete-time optimal control problems. Liao and Shoemaker (1991) also developed similar methods. Coleman and Liao (1995) proposed the thrust region method for solving unconstrained discrete optimal control problems. This method also works for large-scale minimization problems.

Betts (2001) reformulated the original dynamic optimization problem as a non-linear programming (NLP) problem by direct transcription as a static optimization problem. This is achieved by parameterization of the state variables or the control variables or sometimes both. The advantage of this method is that the Hamiltonian formulation can be completely avoided. However, there are some problems with this method. It requires an excessive computing time if it results in a large-scale NLP problem. Numerical stability and convergence problems might also occur. Parameterization might introduce spurious local minima which are not present in the original problem (Crispin, 2007). Global optimization methods can be used to overcome the above-mentioned disadvantages. The global optimization methods include stochastic methods such as simulated annealing (Van Laarhoven and Aarts, 1987), and evolutionary methods such as genetic algorithms (GAs) (Michalewicz, 1992).

Early applications of optimal control problems in the aerospace field were confined to flight trajectory optimization problems. Later, various other aerospace applications have been considered and successfully solved. One application which has not been considered in the literature is hybrid rocket optimization combining with the trajectory optimization using mass flow rate of the oxidizer as control.

1.2. Hybrid Rocket

A hybrid rocket propulsion system uses both liquid and solid propellants. A classical hybrid rocket uses a liquid oxidizer and solid fuel. The operation of the hybrid rocket is different from that of a liquid and a solid rocket, though there are many components common to the liquid and the solid rocket. Although the liquid rocket is a high-performance system, it is quite complex and costly. This problem can be overcome with the solid motor, but the disadvantages of the solid motor are danger of explosion and lack of thrust control. Hybrid rockets provide an attractive alternative option because of their non-explosiveness, simplicity of operation, and low cost. The hybrid burns as a macroscopic turbulent diffusion flame, where the oxidizer to fuel ratio varies down the length of the combustion chamber, ending at a composition that determines the performance of the motor (Chiaverini, 2000).

1.2.1. Advantages of Hybrid Rockets

Safety: The hybrid rocket is inherently safer than the other rocket designs because oxidizer and fuel are stored separately. Also, because the fuel is inert, storage and handling are much simpler.

Throttling and shutdown: The hybrid rocket engine can be throttled to optimize the trajectory during the atmospheric launch and orbital injection by modulating the oxidizer

flow rate. In contrast, this cannot be achieved in a solid and liquid rocket, which requires two flow rates to be synchronized while being modulated. Thrust termination for the hybrid rocket can be accomplished simply by turning off the liquid flow rate.

Low-cost: The operational cost for a hybrid rocket system greatly benefits from the inert and safety features. The system can tolerate larger design margins, resulting in a lower fabrication cost. The system cost can be lowered due to the reduced failure modes, which permits the use of commercial-grade, instead of Mil-spec, ingredients (Larson et al., 1995).

Temperature sensitivity: The concern for a maximum expected operating pressure (MEOP) is greatly reduced because the ambient launch temperature variations have little effect on operating chamber pressure.

Propellant versatility: In contrast to liquids, solid fuel permits the addition of many other ingredients such as energetic metals to enhance both performance and density without slurries.

Grain robustness: One of the tremendous advantages of any hybrid's solid fuel is that the grain cracks are not catastrophic because the burning occurs only in the port where it encounters the oxidizer flow (Altman, 1991).

Environmental Cleanliness: Hybrid rockets with non-metalized fuels do not produce hydrochloric acids, aluminum oxide, and other undesirable product species in the exhaust. Therefore, hybrid rockets have a lesser environmental impact than solid rockets and are at least as environmentally benign as liquid rockets (Larson et al., 1995).

1.2.2. Disadvantages of Hybrid Rockets

There are some disadvantages of hybrid rockets, despite the above advantages. These include:

O/F Shift: At a fixed mass flow rate, there is a tendency for the oxidizer to fuel ratio to shift to higher values as the port opens during the burn. The change of the O/F ratio implies a change in a specific impulse and a possible reduction in vehicle performance.

Low-Regression rate: In classical hybrids, the regression rates of commonly used solid fuels are relatively low in comparison with solid propellants. This imposes constraints on the fuel grain design. However, this characteristic may be an advantage for long-duration applications such as target drones, hovering vehicles, and gas generators.

Combustion Efficiency: The combustion efficiencies of hybrid rockets are low compared to liquid propellant or solid propellant rockets. This is due to the nature of the large diffusion flame resulting in a lower degree of mixing.

Low-Bulk density: The density impulse of hybrid rockets is usually lower than that of solid rockets because we must inject the total oxidizer at the head end and allow for a mixing volume aft of the grain. This results in a lower mass fraction than in liquids or solids.

1.3. Objective

In a hybrid rocket, the mass flow rate of the oxidizer can be controlled to increase the performance of the rocket. Two equivalent problems are considered to enhance the performance of the hybrid rocket by controlling the mass flow rate of the oxidizer.
First, to maximize the altitude reached for a given amount of propellant. Second is to minimize the amount of the propellant required to reach a specific altitude and carry a given amount of payload. A genetic algorithm is used to obtain the optimal solution for the mass flow rate of the oxidizer.

2. Review of the Relevant Literature

In this chapter, we discuss previous work on hybrid rockets and the ascent trajectory optimization. Vonderwell, Murray, and Heister (1995) developed a ballistic model to investigate the influence of fuel-grain design on the overall performance of hybrid rocket boosters. The ballistic model is based on steady, one-dimensional compressible flow, and includes the capability to handle arbitrary wagon-wheel fuel-grain designs. The model has the capability to predict stagnation-pressure losses along the fuel ports and can handle throttling. The optimization is carried out for liquid oxygen and 90% hydrogen peroxide as oxidizers assuming hydroxyl-terminated polybutadiene as fuel. The results obtained indicate that the liquid-oxygen system optimizes to a higher number of ports and the mass flux levels compare to the hydrogen peroxide system.

Schoonover et al., (2000) optimized the design of a large hybrid rocket booster using a genetic algorithm optimization technique. They used a hybrid rocket optimal sizing code developed at Purdue University to minimize the gross lift-off weight or total inert weight. Optimal or near-optimal solutions were obtained for continuous variables such as tank pressure, chamber pressure, and oxidizer mass flow rate, and the discrete variables such as propellant combination and the number of fuel ports, were simultaneously optimized.

Kim and Spencer (2002) used a genetic algorithm to solve the optimal rendezvous of two spacecraft. They obtained the thrust time history that includes the magnitude and the direction of the velocity change, and the burn position such that the boundary conditions are satisfied. This method was used to solve three test cases: 1) the Hohmann transfer 2) the bielliptic transfer and 3) Rendezvous with two impulses. The results for the first two

cases match the analytical solutions; for the rendezvous with two impulse case, the results do not match the analytical solution, but the configuration of the trajectory is similar to the analytical solution.

Casalino and Pastrone (2005) analyzed the effect of design parameters and oxidizer flow rate control of a hybrid rocket for small satellites. The design parameters are optimized to minimize the engine mass, keeping the initial satellite mass and required velocity increment constant. Several control strategies are compared to study the effect of throttling. From the results, the constant mixture ratio control had a large thrust variation, but repressurization control reduced the thrust variation. The constant pressure controls both the combustion chamber pressure and the tank pressure to ensure a quasi- constant thrust and reduce the engine dimensions.

Park, Scheers, and Guibout (2006), proposed a new method based on Hamiltonian – Jacobi theory to evaluate an optimal trajectory and optimal feedback control. A continuous thrust rendezvous problem relative to a circular orbit has been solved using this method. The optimal feedback control and the optimal trajectory are obtained using generating functions, which are developed as series expansions. The optimal trajectories obtained are compared with the numerical solution obtained using a two-point boundary value problem using a forward shooting method. The results obtained imply that this method can be considered as an alternative and effective way of solving non-linear optimal rendezvous problems.

Rhee et al. (2008) conducted a feasibility study of a hybrid rocket motor with HTPB/LOX combination to substitute for the solid rocket motor of the first stage of the Pegasus XL. The optimal design of a hybrid rocket motor was carried out to minimize the

total mass of the vehicle and to minimize the engine length separately to determine which approach is more efficient. The result shows that both approaches provide nearly the same results.

Casalino and Pastrone (2010) optimized a hybrid rocket motor for an upper stage launcher. The design parameters of a hybrid rocket and the trajectory are simultaneously optimized to maximize the payload inserted into a prescribed orbit. The optimal values are obtained for pressurizing gas mass, nozzle expansion ratio, initial value of the tank pressure, mixture ratio, and thrust. The trajectory optimization is carried out by controlling thrust direction. The results obtained show that the hybrid rocket provides better results than the solid or the liquid rocket upper stage launchers.

Casalino and Pastrone (2012) analyzed the performance of single-stage and two-stage hybrid rockets for different payload fractions. They used a multi-disciplinary optimization method, which combines the direct optimization of design parameters and indirect optimization of trajectory to maximize the final Mach number for given initial conditions, assigned payload, and final altitude. The results obtained show that two-stage rockets offer better performance for a small payload fraction and large final velocities.

Rao et al. (2012) designed a two-stage variable thrust hybrid rocket motor for sounding rockets. They developed a computational program to predict the internal ballistics and trajectory. A modified differential evolution algorithm is employed to maximize the payload mass for a star grain and the wheel grain geometries. The computational results indicate that a larger payload mass and a lower length to diameter ratio were obtained for the wheel grain geometry.

Cai et al. (2013) used an optimal design method to optimize the design of a ballistic single-stage sub-orbital hybrid rocket vehicle. The optimal method is based on the multi-island genetic algorithm. The optimization is carried out for different propellant combinations and grain types to analyze the effect of design parameters and the propellant combination on the performance of the hybrid rocket. The results show that the total mass of the vehicle can be reduced by increasing the oxidizer mass concentration. A multi-tube grain performs the best compared to star-port grain, single circular port grain, and wheel port grain because it has the largest burning perimeter length.

Casalino, Pastrone, and Simeoni (2015) introduced different strategies to reduce the computational time required to optimize the upper-stage hybrid rocket. The computational time was reduced by 15-20%, and the robustness of the optimizer was increased by using a multiple-shooting approach. The performance of the previously developed evolutionary algorithm was increased by better formulation of the fitness function.

Casalino, Pastrone and Masseni (2018) optimized a three-stage hybrid rocket with different numbers of engines in each stage for a small-satellite launcher. The trajectory optimization is carried out by controlling the velocity angle on the horizon at first stage ignition in order to maximize the payload mass for a given inert orbit. The results are compared for two designs. In the first one the acceleration at the first stage is fixed, and in the second case, the initial thrust is optimized. The results show that payload is maximum for the second design but requires a constraint on maximum acceleration.

From this literature review, it is observed that the optimization of a hybrid rocket has been carried out to obtain the optimal design parameters such as fuel-grain geometry,

chamber pressure, initial tank pressure, and initial oxidizer to fuel ratio. The trajectory optimization is done by controlling the thrust directly. But, in a hybrid rocket, we cannot control the thrust directly; only the mass flow rate of the oxidizer can be controlled. In the present work, we optimize the internal ballistics and the trajectory together to obtain the optimal mass flow rate of the oxidizer as a function of time to minimize the propellant required to reach a specific altitude for a given mission. First, we solve for optimal control using a genetic algorithm to maximize the altitude for a fixed amount of propellant. Later, we solve for propellant required to reach a specific altitude using the optimal mass flow rate of the oxidizer obtained from the genetic algorithm. We initially considered a simple regression rate equation depending only on the mass flux rate of the oxidizer, then we considered a regression rate equation depending on both the mass flux rate of the oxidizer and the fuel. Next, we present the mathematical formulation for internal ballistics of hybrid rocket, ascent trajectory, and optimal control problems.

3. Internal Ballistics of Hybrid Rocket

In this chapter, we will discuss the internal ballistics of a hybrid rocket engine. The internal ballistics depend on the solid fuel regression rate $\dot{r}$. Initially, we consider a simple regression rate equation depending only on the mass flux rate of the oxidizer, which is given by the expression (Altman, 1991):

$$\dot{r}(t,x) = ax^m G_{ox}^n \tag{3.1}$$

where x is the axial distance from the port entrance, a is the regression rate coefficient, n, m are regression rate exponents and G_{ox} is the oxidizer mass flux rate.

The mass flux rate is defined as the mass flow per unit cross-sectional area. The mass flux rate of the oxidizer is given by:

$$G_{ox} = \frac{\dot{m}_{ox}}{NA_p} \tag{3.2}$$

where, $\dot{m}_{ox}$ is the oxidizer mass flow rate, N is the number of ports and A_p is the area of the port. The mass flux rate of the fuel is given by:

$$G_f = \frac{\dot{m}_f}{NA_p} \tag{3.3}$$

where $\dot{m}_f$ is the fuel mass flow rate.

As the fuel burns, the cross-sectional area of the port A_P increases and the mass flux rate of the propellant varies as a function of time t and axial distance x. The mass flux rate of the propellant G is given by:

$$G(t,x) = G_f(t,x) + G_{ox}(t,x) \tag{3.4}$$

The mass flow rate of the fuel $d\dot{m}_f$ generated in a single port for a small differential area as shown in Figure 3.1between station x and station $x + dx$ is:

$$d\dot{m}_f = \rho_f \dot{r}(t,x) P_p(t,x) dx \tag{3.5}$$

where ρ_f is the density of the fuel, and $P_p(t,x)dx$ is the contact area between the solid fuel and the mixture of reacting gases in the port between station x and station $x + dx$.

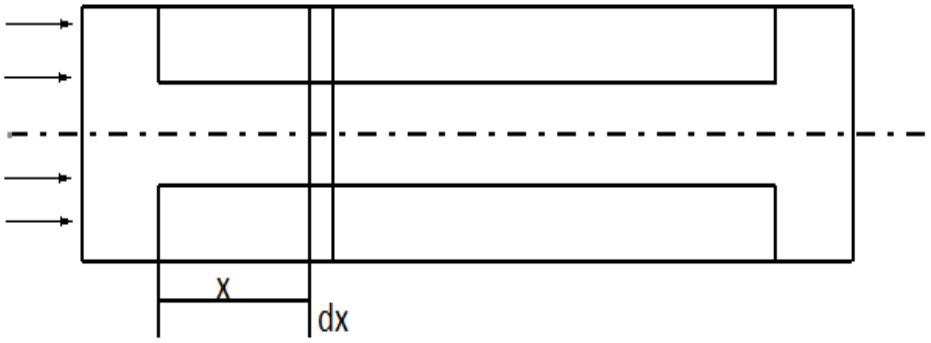

Figure 3.1 Axial cross-section of the solid fuel port

The fuel mass flux rate $G_f(t,x)$ can be obtained by integrating the amount of fuel released from the solid fuel along the axis of the port x. The mass flux rate of the fuel generated between the entrance to the port $x = 0$ and station x is given by:

$$G_f(t,x) = \frac{\int_0^x d\dot{m}_f}{A_p(t,x)} = \frac{\int_0^x \rho_f \dot{r}(t,\xi) P_p(t,\xi) d\xi}{A_p(t,x)} \tag{3.6}$$

The cross-sectional area of the port A_p and the perimeter of the port P_p are given by the following equations in terms of the hydraulic diameter $D_H(t)$.

$$A_p(t) = \frac{\pi D_H^2(t)}{4} \tag{3.7}$$

$$P_p(t) = \pi D_H(t) \tag{3.8}$$

Here we present a simplified model by considering average values of the regression rate and hydraulic diameter along the port axis. We eliminate the dependence of the

regression rate and hydraulic diameter on the coordinate x so that the flux rate $G_f(t,x)$ can be approximated by the following expression.

$$G_f(t) = 4\rho_f \frac{\dot{r}(t)P_p(t)}{A_p(t)} \int_0^{L_p} d\xi = \frac{4\rho_f L_p \dot{r}(t)P_p(t)}{A_p(t)} \tag{3.9}$$

where L_p is the port length. Substituting Equations (3.7) and (3.8) into Equation (3.9), and simplifying we get following equation for the mass flux rate of the oxidizer.

$$G_f(t) = \frac{4\rho_f L_p \dot{r}(t)}{D_H(t)} \tag{3.10}$$

The regression rate can be approximated by:

$$\dot{r}(t) = aL_p^m G_{ox}^n \tag{3.11}$$

Substituting the area of the port Equation (3.7) into the oxidizer mass flux rate Equation (3.2), we obtain:

$$G_{ox}(t) = \frac{4\dot{m}_{ox}(t)}{\pi N D_H^2(t)} \tag{3.12}$$

Substituting the expression for the regression rate $\dot{r}(t)$ and G_{ox} in Equation (3.10), we obtain the equation for the fuel mass flux rate. The propellant mass flow rate is given by Equation (3.14):

$$G_f(t) = 4\rho_f a L_p^{m+1} \frac{1}{D_H(t)} \left[\frac{4\dot{m}_{ox}(t)}{\pi N D_H^2(t)}\right]^n \tag{3.13}$$

$$\dot{m}_p(t) = \dot{m}_{ox}(t) + \dot{m}_f(t) \tag{3.14}$$

The hydraulic diameter at any time t is given by:

$$D_H(t) = D_{H0} + 2w(t) \tag{3.15}$$

where w(t) is the solid fuel web distance at time t and D_{H0} is the initial hydraulic diameter as shown in Figure 3.2.

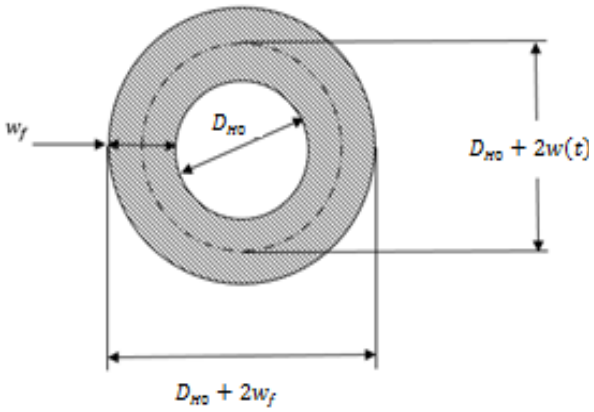

Figure 3.2 Cross-section of a circular port

Taking the derivative of the hydraulic diameter with respect to time we obtain:

$$\frac{dD_H}{dt} = \frac{2dw}{dt} = 2\dot{r}(t) \tag{3.16}$$

$$\frac{dD_H}{dt} = 2aL_p^m G_{ox}^n(t) \tag{3.17}$$

$$\frac{dD_H}{dt} = 2aL_p^m \left[\frac{4\dot{m}_{ox}}{\pi N D_H^2(t)}\right]^n \tag{3.18}$$

We non-dimensionalize the internal ballistics equations by introducing the following non-dimensional parameters.

$$\bar{t} = \frac{t}{\tau}\ ; \qquad \bar{D}_H = \frac{D_H}{D_{H0}}\ ; \qquad \bar{G}_{ox} = \frac{G_{ox}}{G_{ox0}}\ ; \qquad \bar{G}_f = \frac{G_f}{G_{f0}}\ ;$$

$$\bar{\dot{m}}_{ox} = \frac{\dot{m}_{ox}}{\dot{m}_{ox0}}\ ; \qquad \bar{\dot{m}}_f = \frac{\dot{m}_f}{\dot{m}_{f0}}\ ; \qquad \bar{\dot{m}}_p = \frac{\dot{m}_p}{\dot{m}_{p0}}\ ; \qquad (OF)_0 = \frac{G_{ox0}}{G_{f0}};$$

$$\tau = \frac{w_f}{\dot{r}_0}\ ; \qquad \lambda_1 = \frac{w_f}{D_{H0}}; \qquad \dot{r}_0 = aL_p^m G_{ox0}^n\ ; \qquad OF = \frac{G_{ox}}{G_f};$$

where τ is the characteristic time, w_f is the final fuel web thickness, $\dot{r}_0$ is the initial web thickness, D_{H0} is the initial hydraulic diameter, G_{ox0} is the initial oxidizer mass flux rate, G_{f0} is the nitial fuel mass flux rate, $\dot{m}_{ox0}$ is the initial mass flow rate of oxidizer, $\dot{m}_{f0}$ is the initial mass flow rate of fuel, $\dot{m}_{p0}$ is the initial propellant mass flow rate, $(OF)_0$ is the initial oxidizer to fuel ratio, and OF is the oxidizer to fuel ratio.

Substituting the non-dimensional parameters in Equations (3.12), (3.13), (3.14) and (3.18), we obtain following equations:

$$G_{ox}(t)\bar{G}_{ox}(\bar{t}) = \frac{4\dot{m}_{ox0}\bar{\dot{m}}_{ox}(\bar{t})}{\pi N D_{H0}^2 \bar{D}_H^2\,(\bar{t})} \tag{3.19}$$

$$G_{f0}\bar{G}_f(\bar{t}) = \frac{4\rho_f a L_p^{m+1}}{D_{H0}\bar{D}_H(\bar{t})}\left[\frac{4\dot{m}_{ox0}\bar{\dot{m}}_{ox}(\bar{t})}{\pi N D_{H0}^2 \bar{D}_H^2\,(\bar{t})}\right]^n \tag{3.20}$$

$$\dot{m}_{p0}\bar{\dot{m}}_p(\bar{t}) = \dot{m}_{ox0}\bar{\dot{m}}_{ox}(\bar{t}) + \dot{m}_{f0}\bar{\dot{m}}_f(\bar{t}) \tag{3.21}$$

$$\frac{D_{H0}d\bar{D}_H}{\tau d\bar{t}} = 2aL_p^m\left[\frac{4\dot{m}_{ox0}\bar{\dot{m}}_{ox}(\bar{t})}{\pi N D_{H0}^2 \bar{D}_H^2\,(\bar{t})}\right]^n \tag{3.22}$$

By simplifying the above equations, we get the equations for the hydraulic diameter, the mass flux rate of the oxidizer, the mass flux rate of the fuel and the propellant mass flow rate are obtained in non-dimensional form.

$$\bar{G}_{ox}(\bar{t}) = \frac{\bar{\dot{m}}_{ox}(\bar{t})}{\bar{D}_H^2\,(\bar{t})} \tag{3.23}$$

$$\bar{G}_f(\bar{t}) = \frac{1}{\bar{D}_H(\bar{t})}\left[\frac{\bar{\dot{m}}_{ox}(\bar{t})}{\bar{D}_H^2\,(\bar{t})}\right]^n \tag{3.24}$$

$$\bar{\dot{m}}_p(\bar{t}) = \left[\frac{(OF)_0}{(OF)_0 + 1}\right] \bar{\dot{m}}_{ox}(\bar{t}) + \left[\frac{1}{(OF)_0 + 1}\right] \bar{D}_H(\bar{t}) \left[\frac{\bar{\dot{m}}_{ox}(\bar{t})}{\bar{D}_H^2(\bar{t})}\right]^n \tag{3.25}$$

$$\frac{d\bar{D}_H}{d\bar{t}} = 2\lambda_1 \left[\frac{\bar{\dot{m}}_{ox}(\bar{t})}{\bar{D}_H^2(\bar{t})}\right]^n \tag{3.26}$$

The internal ballistics equations are obtained in non-dimensional form. Now we introduce the ascent trajectory equations in non-dimensional form.

4. Ascent Trajectory

In this chapter, we obtain the ascent trajectory equations. Let us consider the case where the rocket is climbing vertically in a constant gravity field, and we are neglecting the effect of aerodynamic drag. Newton's second law of motion can be written as:

$$M(t)a = F(t) - M(t)g \tag{4.1}$$

where F(t) is the thrust force acting on the vehicle, a is the acceleration of vehicle, M(t) is the mass of the vehicle as a function of time, and g is acceleration due to gravity.

The thrust of the rocket engine assuming nozzle exit pressure is equal to the atmospheric pressure, is given by:

$$F(t) = \dot{m}_p(t)u_e \tag{4.2}$$

where $\dot{m}_p(t)$ is propellant mass flow rate given by Equation (3.25), and u_e is the nozzle exit velocity. The equations of motion in differential form can be written as:

$$\frac{dv}{dt} = \frac{\dot{m}_p(t)u_e}{M(t)} - g \tag{4.3}$$

$$\frac{dh}{dt} = v(t) \tag{4.4}$$

where, v is the velocity of the vehicle, and h is the altitude reached by the vehicle. The change in mass of the vehicle with respect to time is given by the following equation.

$$\frac{dM}{dt} = -\dot{m}_p(t) \tag{4.5}$$

The following non-dimensional variables are then introduced to obtain the non-dimensional ascent trajectory equations:

$$\bar{h} = \frac{h}{h_m} \;; \qquad \bar{M} = \frac{M}{M_0} \;; \qquad \bar{v} = \frac{v}{v_c} \;; \qquad v_c = \frac{h_m}{\tau}$$

where h_m is the characteristic altitude, M_0 is the initial mass of the vehicle, and v_c is the characteristic velocity. Substituting the non-dimensional variables in Equations (3.2), (3.3), and (3.4) we obtain:

$$\frac{v_c d\bar{v}}{\tau d\bar{t}} = \frac{\dot{m}_{p0}\bar{\dot{m}}_p(\bar{t})u_e}{M_0\bar{M}(\bar{t})} - \frac{g\tau}{v_c} \tag{4.6}$$

$$\frac{h_m d\bar{h}}{\tau d\bar{t}} = v_c\bar{v} \tag{4.7}$$

$$\frac{M_o d\bar{M}}{\tau d\bar{t}} = -\dot{m}_{p0}\bar{\dot{m}}_p(\bar{t}) \tag{4.8}$$

By simplifying Equations (4.6), (4.7), and (4.8) The ascent trajectory equations in non-dimensional form are obtained.

$$\frac{d\bar{v}}{d\bar{t}} = \delta_1 \frac{\bar{\dot{m}}_p(\bar{t})}{\bar{M}(\bar{t})} - \delta_2 \tag{4.9}$$

$$\delta_1 = \frac{\dot{m}_{p0}\tau u_e}{M_0 v_c}; \qquad \delta_2 = \frac{g\tau}{v_c};$$

$$\frac{d\bar{h}}{d\bar{t}} = \bar{v} \tag{4.10}$$

$$\frac{d\bar{M}}{d\bar{t}} = -\bar{\dot{m}}_p(\bar{t})\frac{\dot{m}_{p0}\tau}{M_o} \tag{4.11}$$

We now have internal ballistics and ascent trajectory equations in non-dimensional form. These equations are coupled non-linear algebraic equations. We cannot solve these equations analytically. Therefore, we implement Runge-Kutta-4 method to solve these equations numerically.

5. Initial Sizing of the Hybrid Rocket

To solve the internal ballistics and ascent trajectory equations numerically, we consider a rocket vehicle similar to Spaceship I with Hydroxyl terminated poly butadiene (HTPB) as solid fuel and Nitrous tetroxide (N_2O_4) as liquid oxidizer. We consider following parameters.

Total mass of the vehicle M_0 = 3600 Kg.

Propellant mass M_p = 1900 Kg.

The optimal specific impulse for the propellant combination of HTPB/ N_2O_4 is 297s at an oxidizer to fuel ratio (O/F) of 3.12. So, we use this O/F ratio for sizing the rocket. Mass of the propellant M_p , oxidizer to fuel ratio O/F, mass of the fuel and the mass of the oxidizer are obtained using Equations (5.1), (5.2), (5.3), and (5.4) respectively.

$$M_p = M_{ox} + M_f \tag{5.1}$$

$$O/F = \frac{M_{ox}}{M_f} \tag{5.2}$$

$$M_f = \frac{M_p}{1 + (O/F)} \tag{5.3}$$

$$M_{ox} = \frac{M_p(O/F)}{1 + (O/F)} \tag{5.4}$$

The required volumes of the fuel and the oxidizer can be determined using the following equations:

$$V_f = \frac{M_f}{\rho_f}; \qquad V_{ox} = \frac{M_{ox}}{\rho_{ox}}; \tag{5.5}$$

where V_f is volume of the fuel, ρ_f is density of the fuel, V_{ox} is volume of the oxidizer, and ρ_{ox} is density of the oxidizer,

In this case, we are considering a 7- circular port geometry. The required fuel volume per port is given by:

$$V_{fp} = \frac{V_f}{7} \tag{5.6}$$

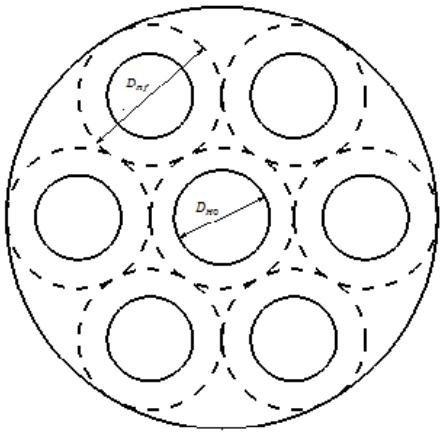

Figure 5.1 Cross-section of a seven circular port geometry

Now, we obtain the size of the circular fuel ports as we have the volume of the fuel per port. We consider the burn time to be 80 sec. First, we estimate the mass flow rate of fuel and oxidizer through all the ports.

$$\dot{m}_{ox} = \frac{M_{ox}}{t_b} \tag{5.7}$$

$$\dot{m}_f = \frac{M_f}{t_b} \tag{5.8}$$

The initial mass flux rate of the oxidizer G_{oxo}, and fuel G_{fo} are given by the following equations.

$$G_{oxo} = \frac{\dot{m}_{ox}}{NA_{p0}} \tag{5.9}$$

$$G_{f0} = \frac{\dot{m}_f}{NA_{p0}} \tag{5.10}$$

where A_{p0} is the initial area of the port and is given by:

$$A_{p0} = \frac{\pi}{4} D_{P0}^2 \tag{5.11}$$

To determine the initial port diameter D_{P0}, we considered the initial mass flux rate of the oxidizer G_{ox0} to be 350 Kg/ m^2 s (Humble) and solve equations (5.8) and (5.9).

The solid fuel thickness or the web thickness w_f can be estimated using average regression rate $\dot{r}_{av}$ and the burn time t_b.

$$w_f \approx \dot{r}_{av} t_b \tag{5.12}$$

As the burn progresses, the cross-sectional area of the port increases. Therefore, the mass flux rate of the oxidizer and the fuel will decrease. So, we estimate the final regression rate $\dot{r}_f$ to be about one-quarter of the initial regression rate $\dot{r}_0$. The average regression rate and the final the final diameter of the port are obtained using Equations (5.13) and (5.14)

$$\dot{r}_{av} = \frac{\dot{r}_0 + \dot{r}_f}{2} = \frac{5}{8}\dot{r}_0 \tag{5.13}$$

$$D_{pf} = D_{p0} + 2w_f \tag{5.14}$$

We have the values of the initial and the final diameters of the port, so we can obtain the cross-sectional area A_{sf} of the solid fuel for one port.

$$A_{sf} = \frac{\pi}{4}(D_{pf}^2 - D_{p0}^2) \tag{5.15}$$

The length of the port can be estimated using following equation.

$$L_p = \frac{V_{fp}}{A_{sf}} \tag{5.16}$$

Table 5.1

Initial Sizing of hybrid rocket.

Hybrid Rocket Design Parameters	
Total mass of the vehicle (M_0)	3600 Kg
Propellant mass (M_p)	1900 Kg
Initial oxidizer to fuel ratio (OF_0)	3.12
Mass of the fuel (M_f)	461.17 Kg
Mass of the oxidizer (M_{ox})	1438.8 Kg
Density of the fuel (ρ_f)	930 Kg/m^3
Density of the oxidizer (ρ_{ox})	1440 Kg/m^3
Liquid oxidizer volume (V_{ox})	1 m^3
Fuel volume (V_f)	0.5 m^3
Number of ports (N)	7
Fuel Volume per port (V_{fp})	0.07086 m^3
Burn time (t_b)	80 sec
Average oxidizer mass flow rate ($\dot{m}_{ox\_av}$)	18 Kg/s
Average fuel mass flow rate($\dot{m}_{f\_av}$)	5.76 Kg/s
Initial mass flux rate of the oxidizer (G_{ox0})	350 Kg/m^2 s
Initial port diameter (D_{p0})	0.0967 m
Initial mass flux rate of the fuel (G_{f0})	112 Kg/m^2 s

Initial Regression rate ($\dot{r}_0$)	0.19 cm/s
Average regression rate ($\dot{r}_{av}$)	0.12 cm/s
Solid fuel thickness (W_f)	0.096 m
Final diameter of the port (D_{pf})	0.029 m
Cross-sectional area of solid fuel port (A_{sf})	587 cm^2
Length of the port (L_p)	1.2 m

6. Effect of Throttling

We solve the internal ballistics and ascent trajectory equations numerically for the rocket engine size obtained from initial sizing. To study the effect of throttling, we solve differential equations considering different oxidizer mass flow rate controls and compare the results obtained.

6.1. Constant Oxidizer Mass Flow Rate

Initially we consider a constant oxidizer mass flow rate as shown in Figure 6.1. The maximum altitude reached is calculated using total energy at burn out. Figure 6.2 shows that the non-dimensional altitude is 0.793, as we are considering the characteristic altitude to be 100 Km. The altitude reached for this case is 79.03 Km. The mass flow rate of the fuel decreases with respect time as the area of the port is increasing. The propellant mass flow rate also decreases. Oxidizer to fuel ratio is increases as shown in Figure 6.5. The thrust is decreasing with respect to time.

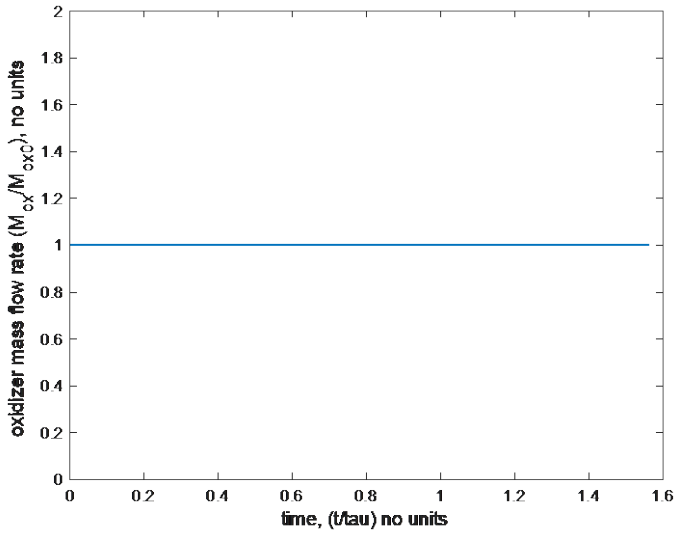

Figure 6.1 Constant oxidizer mass flow rate.

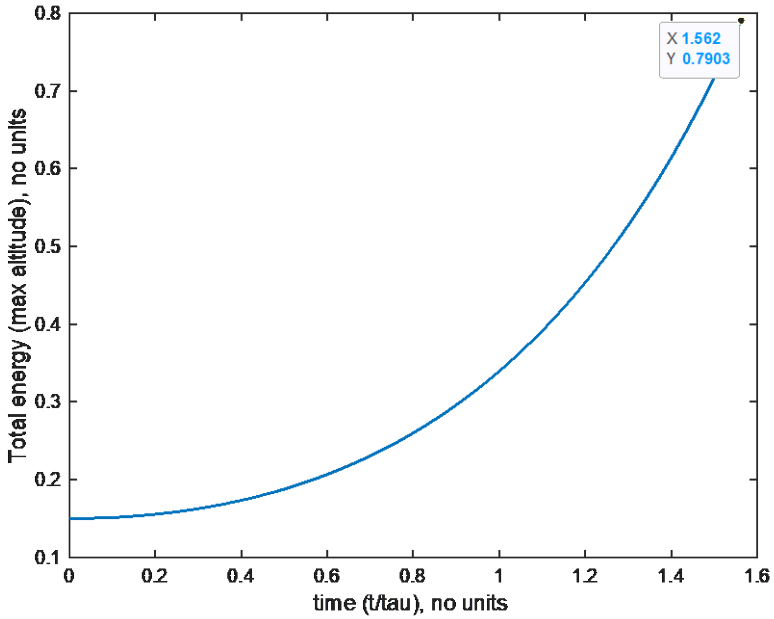

Figure 6.2 Total energy as a function of time for constant oxidizer mass flow rate (total energy at burn time gives the maximum altitude reached).

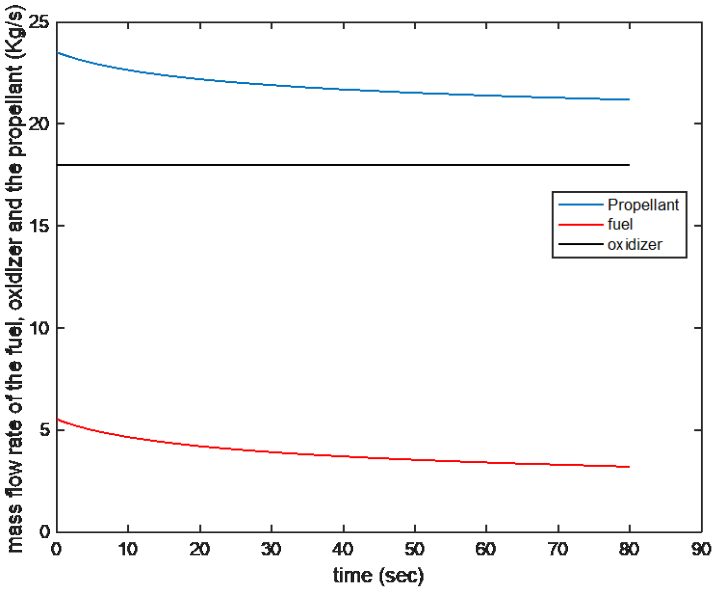

Figure 6.3 Mass flow rate of the oxidizer, the fuel, and the propellant as a function of time.

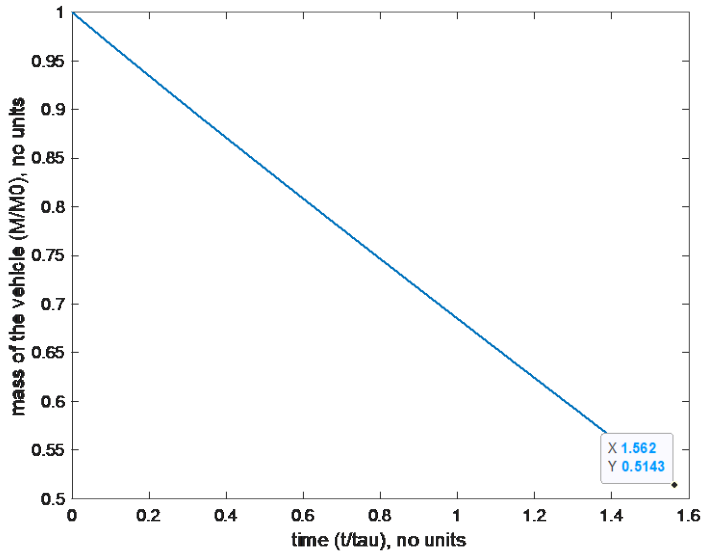

Figure 6.4 Mass of the vehicle as a function of time when the mass flow rate of the oxidizer is constant.

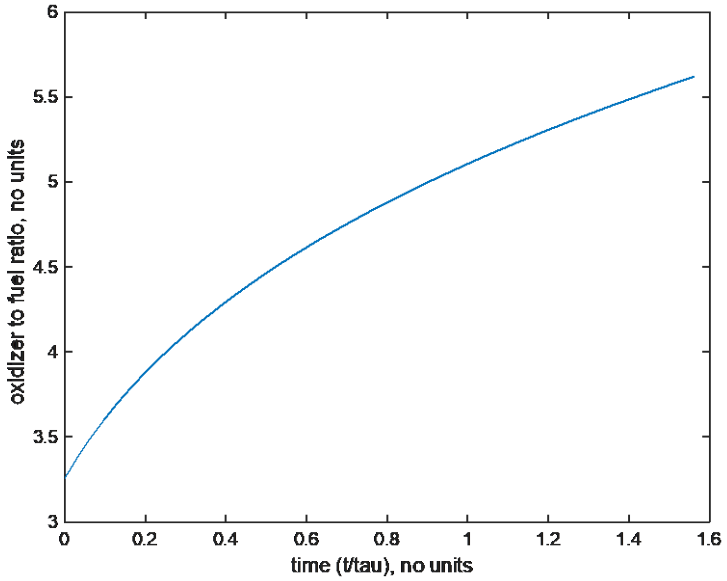

Figure 6.5 Oxidizer to fuel ratio for constant mass flow rate of the oxidizer case.

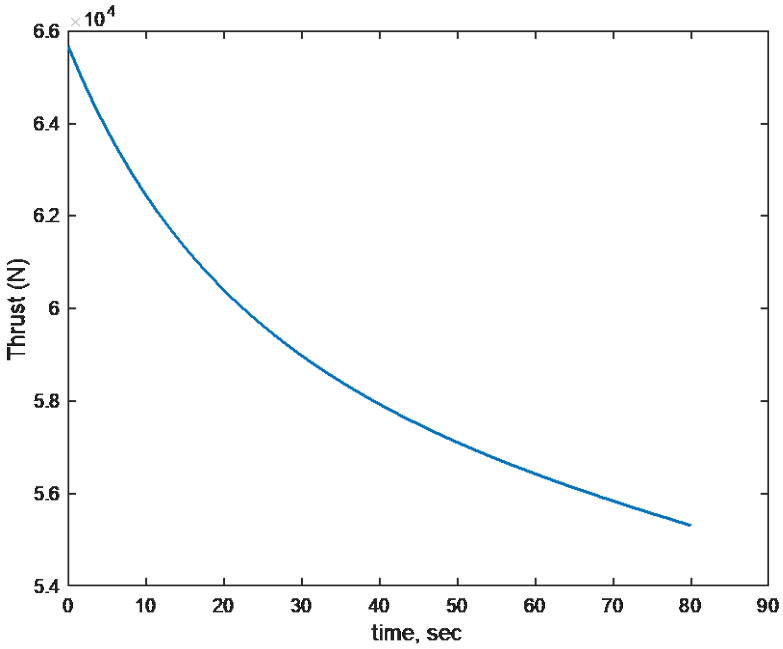

Figure 6.6 Thrust as a function of time for constant mass flow rate of the oxidizer case.

6.2. Linearly Increasing Oxidizer Mass Flow Rate

We consider linearly increasing the oxidizer mass flow rate such that mass of the oxidizer remain same as the previous case. Initially, the mass flow rate of the oxidizer is kept 30% lower than the average mass flow rate of the oxidizer and then linearly increased to a maximum value of 30% higher than the average mass flow rate of the oxidizer. The altitude reached for this case is 72.8 Km. Thrust is increasing linearly, as shown in Figure 6.12, as the mass flow rate of the propellant is also increasing linearly with respect to time. The mass flow rate of the fuel remains almost constant.

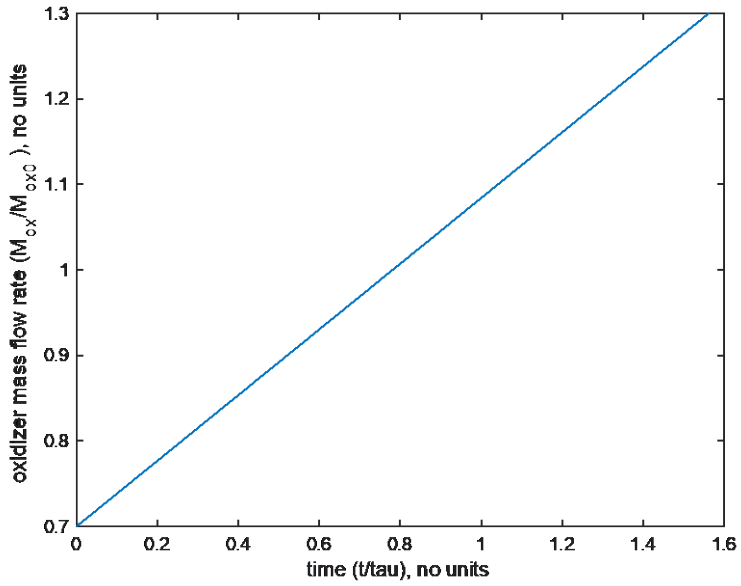

Figure 6.7 Linearly increasing mass flow rate of the oxidizer.

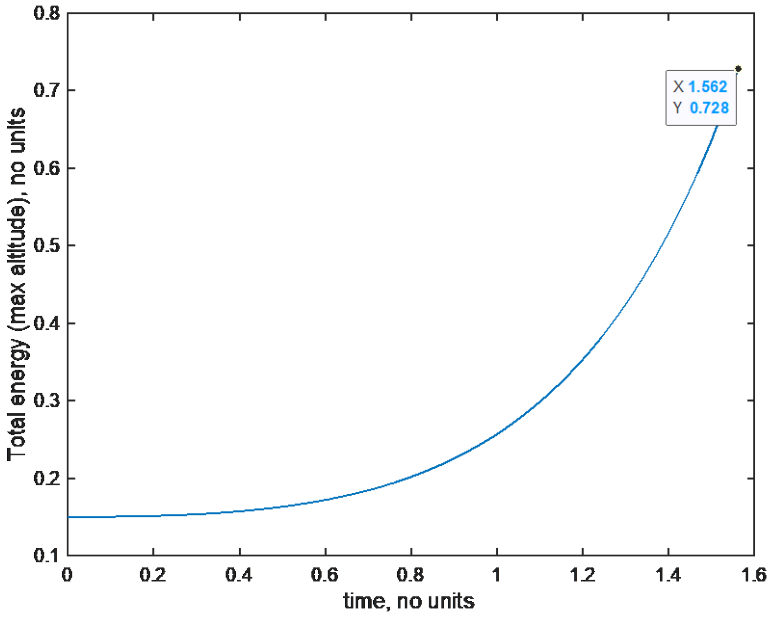

Figure 6.8 Total energy as a function of time for linearly increasing oxidizer mass flow rate (total energy at burn time gives the maximum altitude reached).

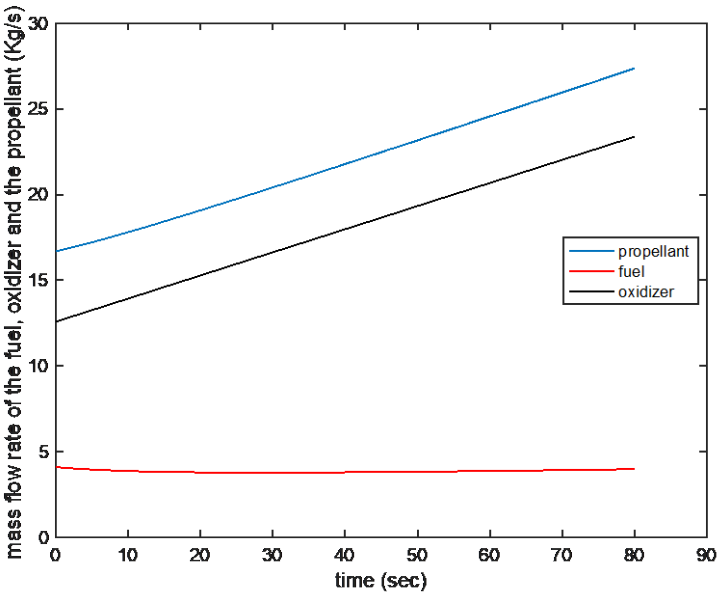

Figure 6.9 Mass flow rate of the oxidizer, the fuel, and the propellant.

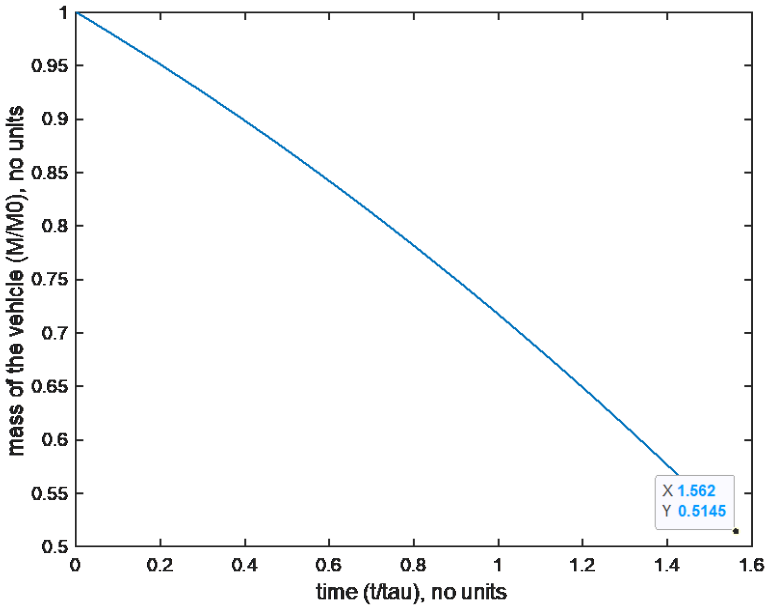

Figure 6.10 Mass of the vehicle as a function of time when mass flow rate of the oxidizer is linearly increasing.

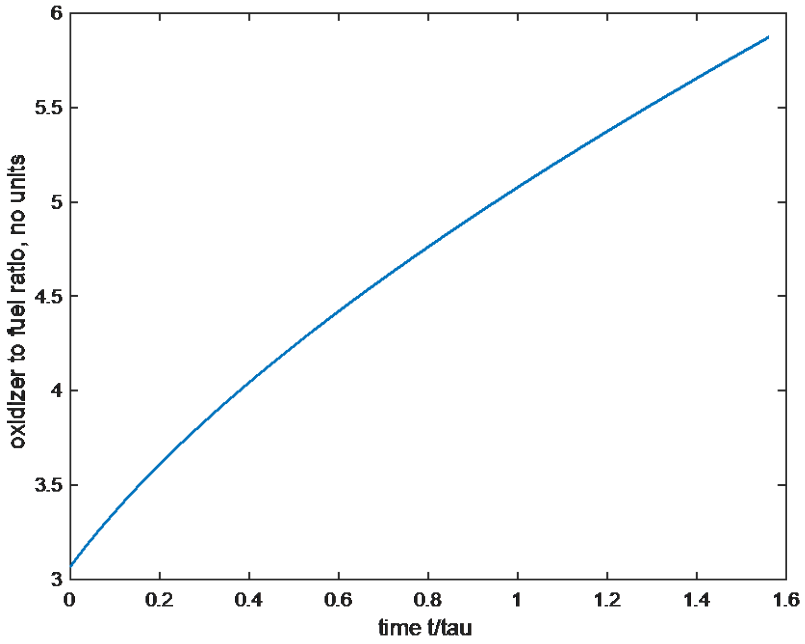

Figure 6.11 Oxidizer to fuel ratio for linearly increasing mass flow rate of the oxidizer case.

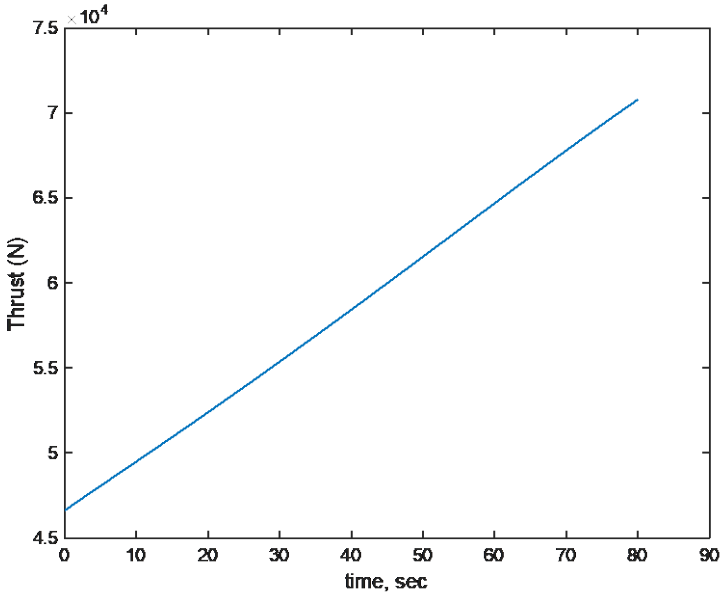

Figure 6.12 Thrust as a function of time when mass flow rate of the oxidizer is linearly increasing.

6.3. Linearly Decreasing Oxidizer Mass Flow Rate

We consider linearly decreasing the oxidizer mass flow rate such that the mass of the oxidizer remains the same as the previous cases. Initially, the mass flow rate of the oxidizer is kept 30% higher than the average mass flow rate of the oxidizer and then linearly decreased to a maximum value of 30% lower than the average mass flow rate of the oxidizer. The altitude reached for this case is 85.31 Km. Figure 6.18 shows that the thrust is decreasing with respect to time. The mass flow rate of the propellant and the fuel are also decreasing with respect to time as shown in Figure 6.15.

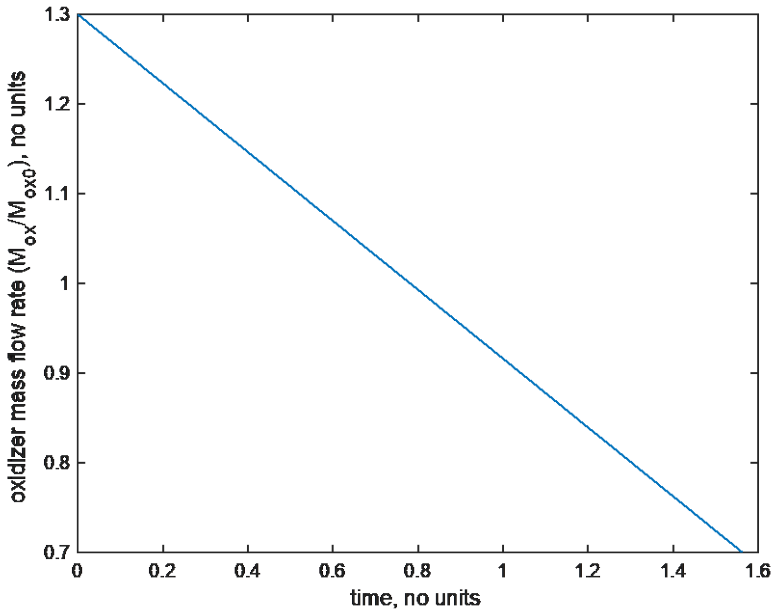

Figure 6.13 Linearly decreasing mass flow rate of the oxidizer.

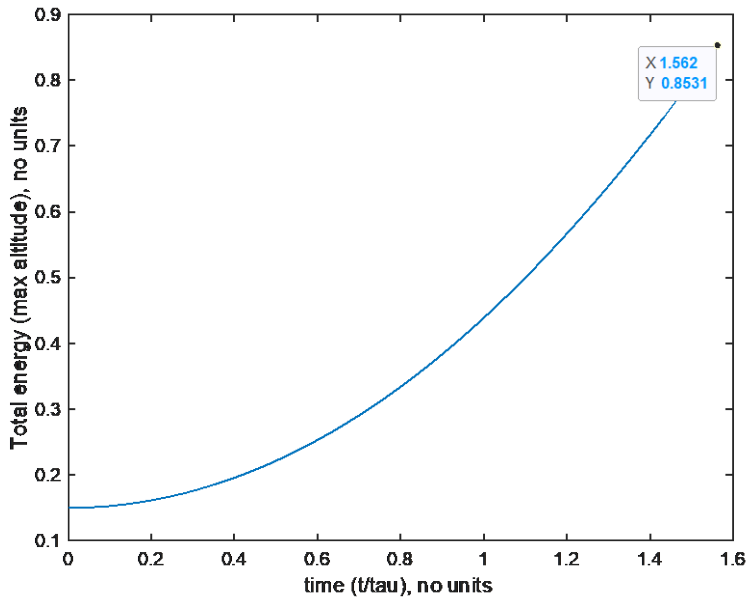

Figure 6.14 Total energy as a function of time for linearly decreasing oxidizer mass flow rate (total energy at burn time gives the maximum altitude reached).

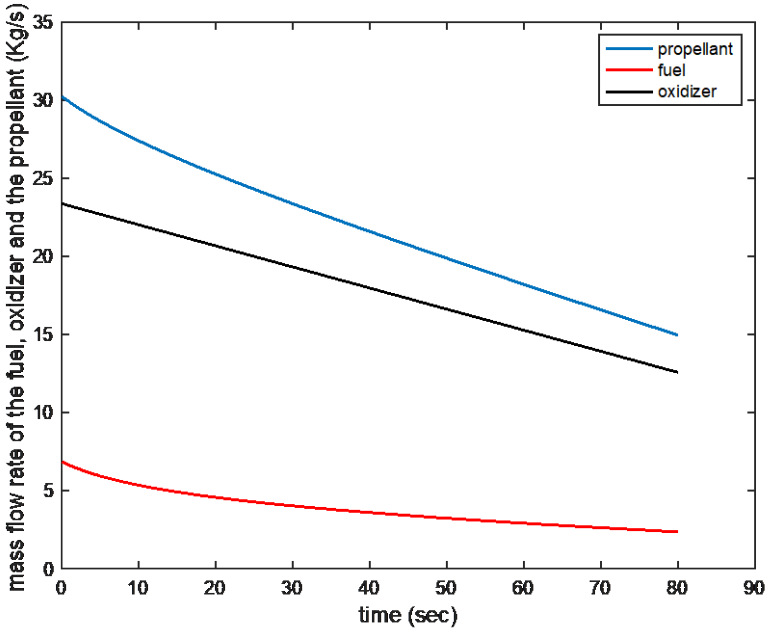

Figure 6.15 Mass flow rate of the oxidizer, the fuel, and the propellant.

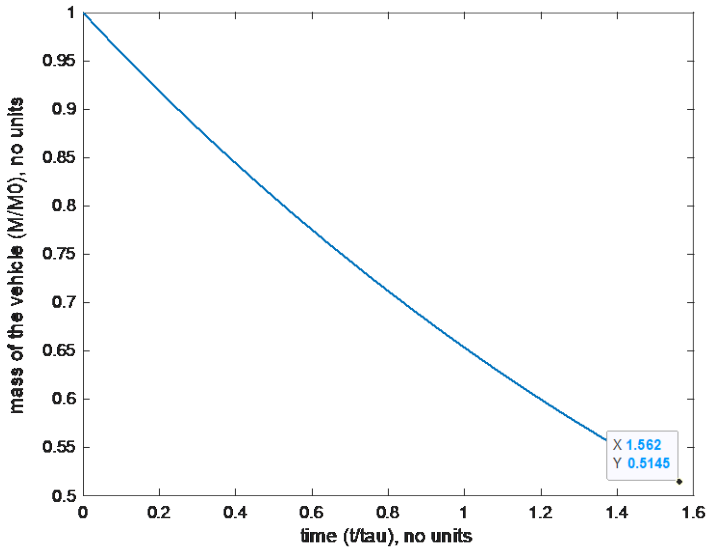

Figure 6.16 Mass of the vehicle as a function of time when mass flow rate of the oxidizer is linearly decreasing.

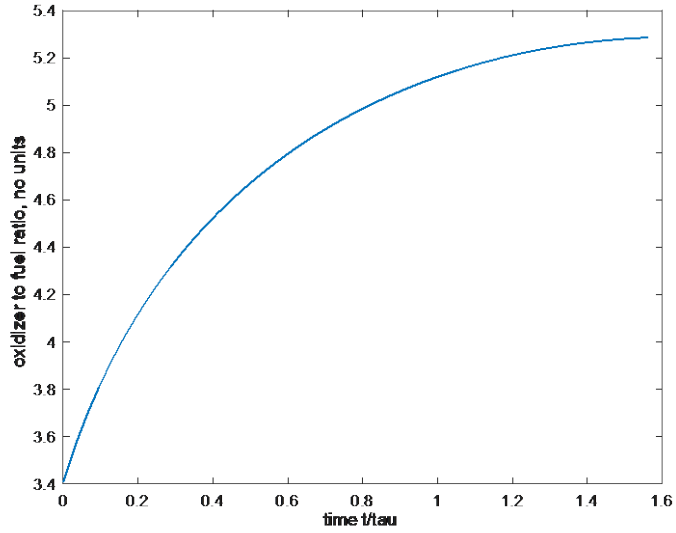

Figure 6.17 Oxidizer to fuel ratio for linearly decreasing mass flow rate of the oxidizer case.

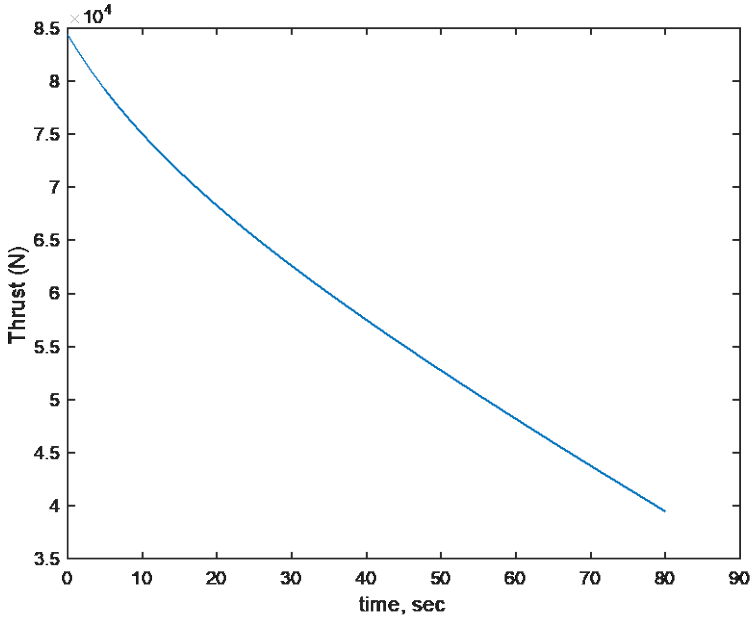

Figure 6.18 Thrust as a function of time when mass flow rate of the oxidizer is linearly decreasing.

From the above results, we can conclude that by throttling, the performance of a hybrid rocket can be improved. To obtain an optimal solution for mass flow rate of the oxidizer, we use a genetic algorithm for optimal control problems. It is also observed that the fuel is not completely burnt because of the oxidizer to fuel ratio we considered for initial sizing. We can also obtain the optimal size of the rocket engine by using the optimal control solution obtained from genetic algorithm.

7. Optimal Control Method and Sizing

We know from previous results that by controlling the mass flow rate of the oxidizer hybrid rocket performance can be enhanced. Now, we implement an optimal control method using a genetic algorithm to obtain the optimal solution for mass flow rate of the oxidizer.

7.1. Problem Formulation

7.1.1. Dynamic Equations

The dynamic equations for this problem are given by the following equations:

$$\frac{d\bar{D}_H}{d\bar{t}} = 2\lambda_1 \left[\frac{\bar{\dot{m}}_{ox}(\bar{t})}{\bar{D}_H^2(\bar{t})} \right]^n \tag{7.1}$$

$$\frac{d\bar{h}}{d\bar{t}} = \bar{v} \tag{7.2}$$

$$\frac{d\bar{v}}{d\bar{t}} = \delta_1 \frac{\bar{\dot{m}}_p(\bar{t})}{\bar{M}(\bar{t})} - \delta_2 \tag{7.3}$$

$$\frac{d\bar{M}}{d\bar{t}} = -\bar{\dot{m}}_p(\bar{t}) \frac{\dot{m}_{p0}\tau}{M_o} \tag{7.4}$$

7.1.2. Fitness Function

The genetic algorithm requires to define a fitness function in order to compare the various members of the population and choose the best control function. In this case the fitness function is altitude and is given by energy at burnout. As the fitness function is not given explicitly, we cannot solve the function analytically. To obtain the optimal control solution, we integrate the dynamic equations using an initial value problem approach and evaluate the fitness function for each member of the population.

We define the objective function, which is given by total energy at any time.

$$J(t) = M(t)gh(t) + \frac{1}{2}M(t)v(t)^2 \tag{7.5}$$

The minimization function or the fitness function to reach the maximum altitude is given by the energy at burn out.

$$J(t_b) = -\left(M(t_b)gh_b + \frac{1}{2}M(t_b)v_b^2\right) \tag{7.6}$$

where h_b is the altitude at burn time, and v_b is the velocity at the burn time. The fitness function in non-dimensional form is given by

$$\bar{J}(t_b) = -\left(\bar{h}_b + \frac{\bar{v}_b^2 v_c^2}{2gh_m}\right) \tag{7.7}$$

7.1.3. Terminal Conditions

We define a terminal condition in terms of total mass of the vehicle at burn out which will ensure that the entire propellant is consumed.

$$\overline{M}(\bar{t}_b) = 1 - \overline{m}_p(\bar{t}_b) = 0.472 \tag{7.8}$$

7.1.4. Optimality Conditions

We obtain the necessary conditions for the optimal solution using Pontryagin's maximum principle.

The Hamiltonian function is given by:

$$H\left(\lambda,\ \bar{h}, \bar{v}, \overline{m}, \overline{D}_H\right) = \lambda_{\bar{h}}\,\bar{v} + \lambda_{\bar{v}}\left(\delta_1 \frac{\dot{\overline{m}}_p(\bar{t})}{\overline{M}(\bar{t})} - \delta_2\right)$$

$$+\lambda_{\overline{m}}\left(-\dot{\overline{m}}_p(\bar{t})\frac{\dot{m}_{p0}\tau}{M_o}\right) + \lambda_{\overline{D}_H}\left(2\lambda_1\left[\frac{\dot{\overline{m}}_{ox}(\bar{t})}{\overline{D}_H^2(\bar{t})}\right]^n\right) \tag{7.9}$$

The Hamiltonian minimization condition (the stationary condition) is given by the derivative of Hamiltonian function with respect to the control input:

$$\frac{\partial H}{\partial \bar{\dot{m}}_{ox}} = \frac{\lambda_{\bar{v}}\delta_1\alpha}{\bar{M}(\bar{t})} - \frac{\lambda_{\bar{m}}\dot{m}_{p0}\tau\alpha}{M_o} + \left[\frac{\bar{\dot{m}}_{ox}(\bar{t})}{\bar{D}_H^2(\bar{t})}\right]^{n-1}\left[\frac{\lambda_{\bar{v}}\delta_1\beta n}{\bar{M}(\bar{t})} - \frac{n\lambda_{\bar{m}}\dot{m}_{p0}\tau\beta}{M_o} + \frac{2\lambda_{\bar{D}_H}\lambda_1}{\bar{D}_H(\bar{t})}\right] = 0 \tag{7.10}$$

where λ are the costates and are obtained by integrating following equations:

$$\lambda = \begin{bmatrix} \lambda_{\bar{h}} \\ \lambda_{\bar{v}} \\ \lambda_{\bar{m}} \\ \lambda_{\bar{D}_H} \end{bmatrix}; \qquad \begin{aligned} -\dot{\lambda}_{\bar{h}} &= \partial_{\bar{h}} H(\lambda,\ \bar{h}, \bar{v}, \bar{M}, \bar{D}_H) \\ -\dot{\lambda}_{\bar{v}} &= \partial_{\bar{v}} H(\lambda,\ \bar{h}, \bar{v}, \bar{M}, \bar{D}_H) \\ -\dot{\lambda}_{\bar{m}} &= \partial_{\bar{m}} H(\lambda,\ \bar{h}, \bar{v}, \bar{M}, \bar{D}_H) \\ -\dot{\lambda}_{\bar{D}_H} &= \partial_{\bar{D}_H} H(\lambda,\ \bar{h}, \bar{v}, \bar{M}, \bar{D}_H) \end{aligned} \tag{7.11}$$

Solving these equations lead to a two-point boundary value problem, which are difficult to solve. To avoid solving TPBVP, we implement a direct search method which is genetic algorithm to solve for optimal solution.

7.2. Genetic Algorithms

Genetic algorithms are heuristic methods used to generate approximate solutions to optimization and search problems by relying on biologically inspired operators such as mutation, crossover, and selection. A typical genetic algorithm requires:

1. A genetic representation of the solution domain
2. A fitness function to evaluate the solution domain

After defining the genetic representation and the fitness function, the genetic algorithm proceeds to initialize the population and then improve it using genetic operators.

7.2.1. Initialization

The initial population is generated randomly, allowing the entire range of possible solutions. The population size depends on the nature of the problem.

7.2.2. Evaluation:

The individual population is evaluated using the fitness function to determine the fitness of the individual.

7.2.3. Selection:

The fittest individuals are selected for reproduction.

7.2.4. Reproduction:

The new population is generated using genetic operators such as crossover and mutation. The fitness function will be evaluated for the new population.

7.2.5. Termination:

This generational process is repeated until the population has converged, or the termination condition has been reached.

7.2.6. Advantages of Genetic Algorithms:

In this approach, the need to solve a difficult two-point boundary-value problem can be avoided. The optimal solution obtained can be verified by solving the necessary conditions for an optimal solution. The functions which are not continuous can also be solved using this method.

7.2.7. Disadvantages of Genetic Algorithms:

In many cases, the convergence of genetic algorithms is very slow. Sometimes the solution converges to a local minimum instead of a global minimum.

7.3. Results from Genetic Algorithms

The results obtained from the genetic algorithm show that the optimal mass flow rate of the oxidizer should be constant at the maximum which is constrained to be 30% higher than the average oxidizer mass flow rate until about one third of the burn time and then

gradually decreased to the minimum, which is constrained to be 30% lower than the average oxidizer mass flow rate. The maximum non-dimensional altitude reached in this case is 1.236 which is 123.6 Km. The results also show that the entire amount of propellant is used.

The optimal mass flow rate of the oxidizer is obtained to maximize the altitude reached for a given amount of propellant. Using mass flow rate of the oxidizer obtained from the genetic algorithm, we minimize the propellant required to reach a specific altitude.

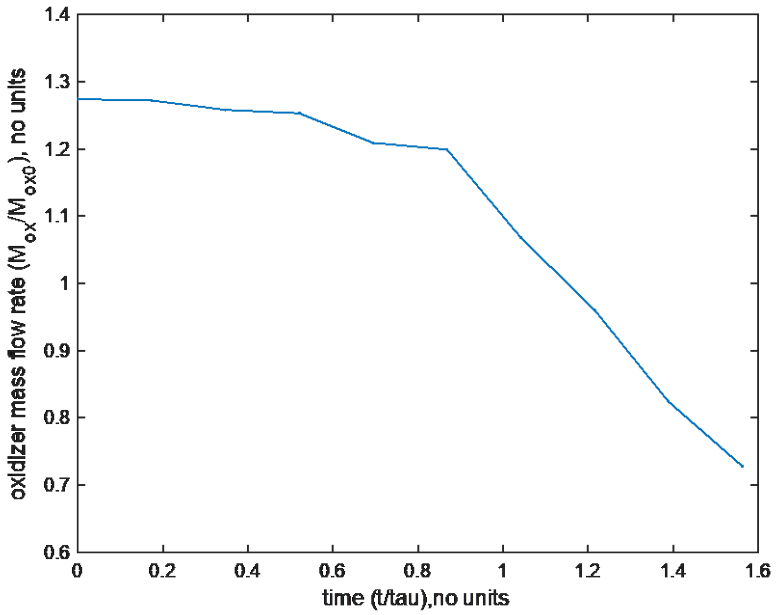

Figure 7.19 Mass flow rate of the oxidizer as a function of time obtained from genetic algorithm.

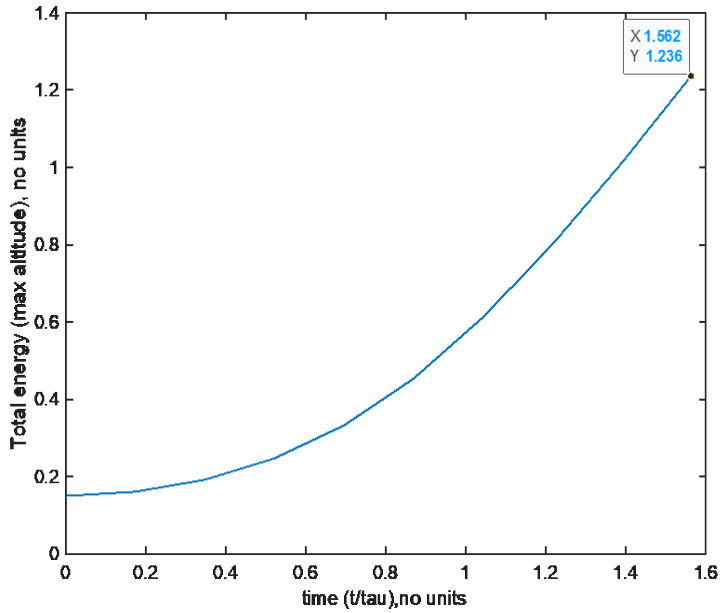

Figure 7.20 Total energy with respect to time for mass flow rate of the oxidizer obtained from genetic algorithm (total energy at burn time gives the maximum altitude reached).

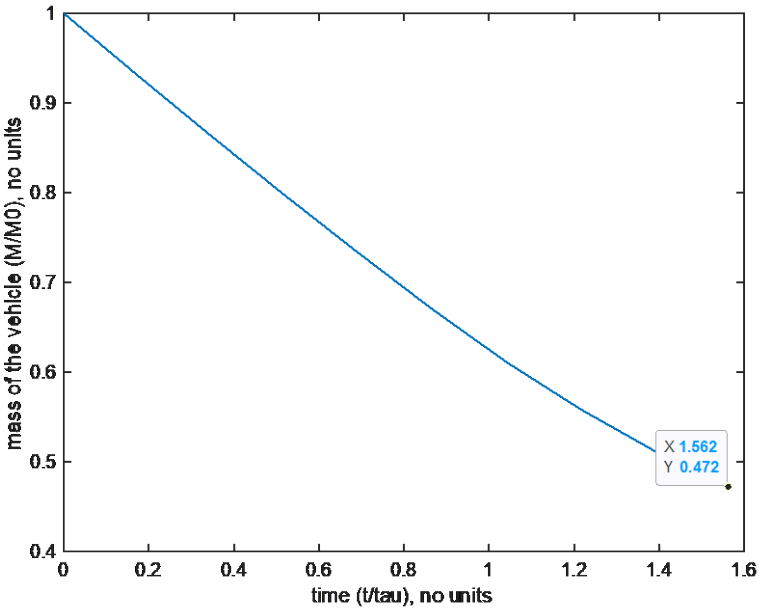

Figure 7.21 Mass of the vehicle as a function of time for optimal mass flow rate of the oxidizer obtained from genetic algorithm.

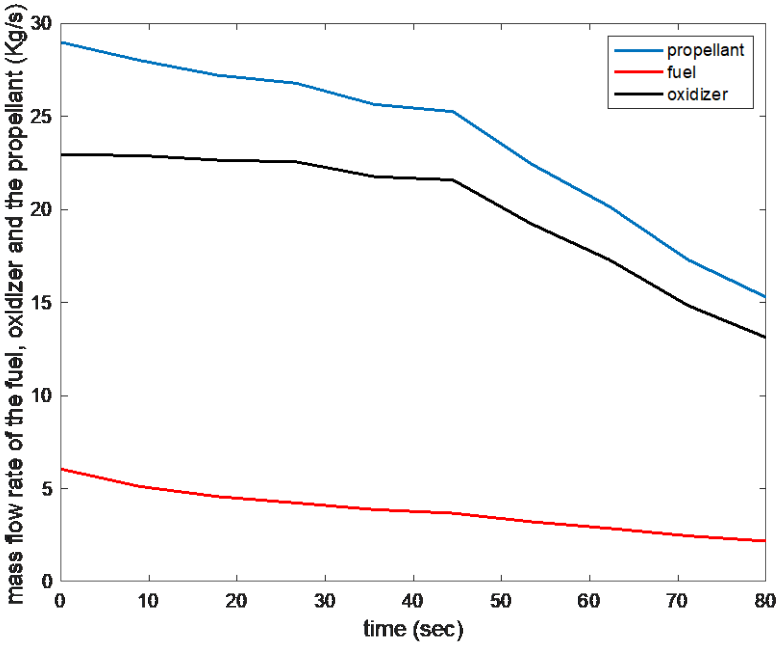

Figure 7.22 Mass flow rate of the oxidizer, the fuel, and the propellant obtained from genetic algorithm.

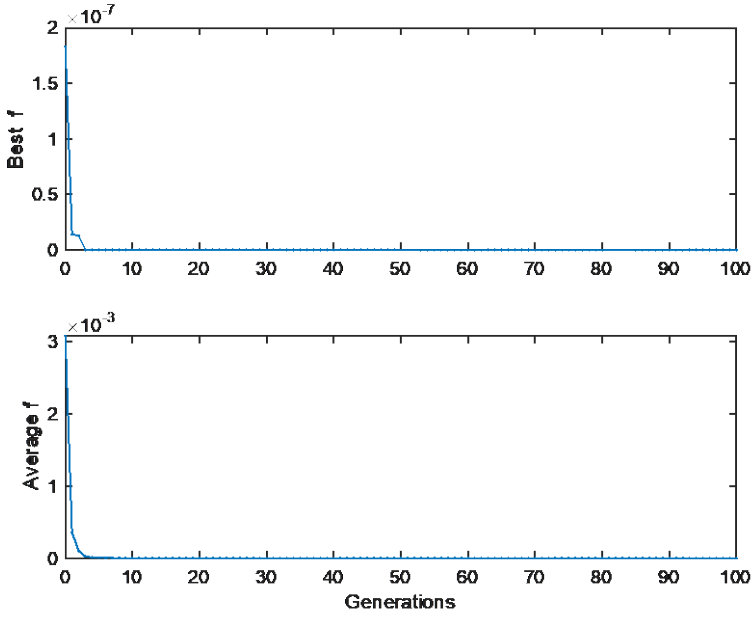

Figure 7.23 Genetic algorithm convergence of fitness function.

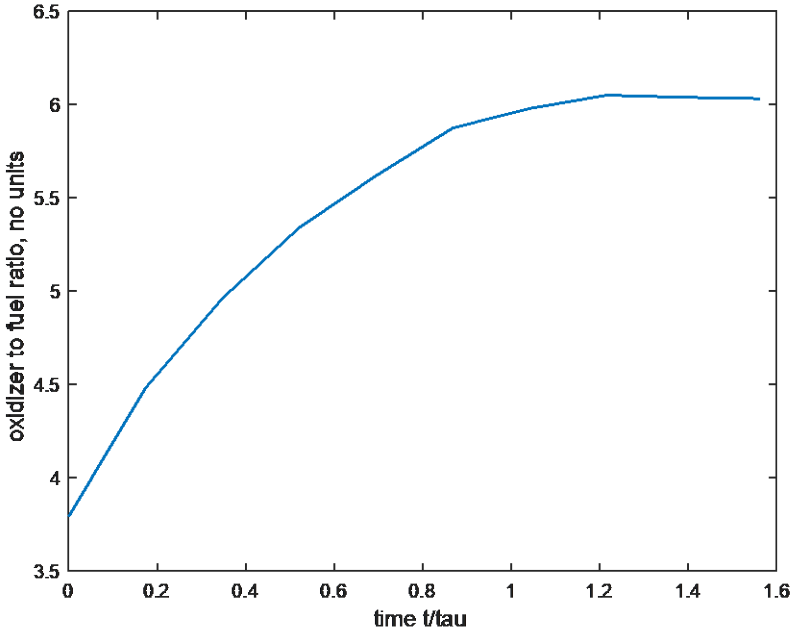

Figure 7.24 Oxidizer to fuel ratio for optimal mass flow rate of the oxidizer.

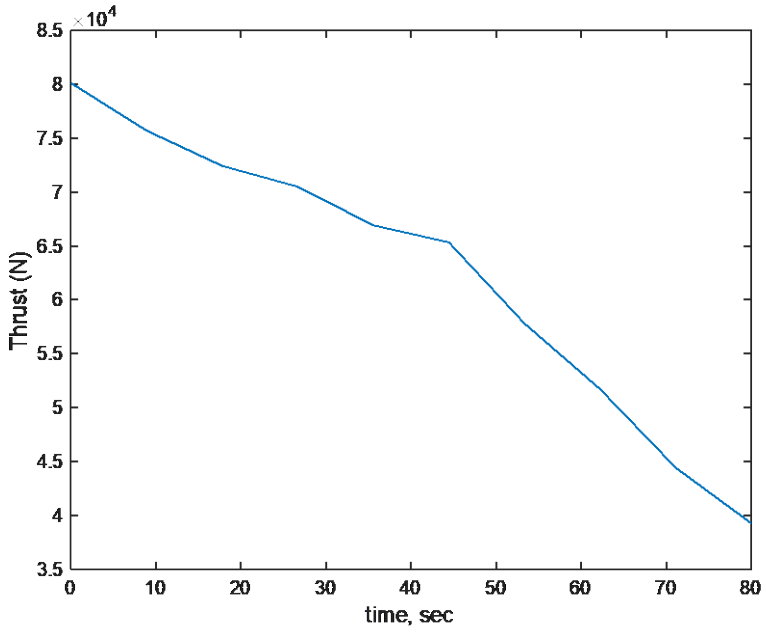

Figure 7.25 Thrust as a function of time for optimal mass flow rate of the oxidizer.

7.4. Optimal Sizing

In Chapter 6, we observed that the fuel is not burned completely for the given amount of oxidizer. That is because of the initial oxidizer to fuel ratio we considered for sizing. To obtain the optimal size of the rocket, we use the oxidizer to fuel ratio obtained from the genetic algorithm.

The optimal mass flow rate of the oxidizer is obtained from the genetic algorithm. The genetic algorithm is a heuristic method, and it gives approximate solution to optimal control problems. We consider three different oxidizer mass flow rates similar to the solution obtained from the genetic algorithm and a baseline case to compare the results: 1) Constant mass flow rate of the oxidizer; 2) Polynomial approximation of the solution obtained from the genetic algorithm; 3) Constant mass flow rate of the oxidizer until about one third of the burn time and then gradually decreasing; and 4) Maximum oxidizer mass flow rate until half of the burn time and then minimum flow rate until end of the burn time, which is a bang-bang control.

Initially, we consider the propellant mass and the initial oxidizer to fuel ratio. For these values we obtain the mass of the oxidizer and the fuel. Then the volume of the oxidizer, the fuel, and the volume of the fuel per port are calculated. The average mass flow rates of the oxidizer and the fuel are obtained by considering burn time to be 80s. The initial port diameter is calculated from the initial mass flux rate of the fuel. The length of the port is estimated to calculate the initial regression rate, average regression rate, fuel web thickness, and the final diameter of the port. The initial value problem of internal ballistics and the ascent trajectory are numerically solved. If the altitude reached

is 100 km, the process will be stopped: if not, the propellant mass and the initial OF ratio will be changed and the process will be repeated.

Table 7.1

Optimal Sizing Methodology.

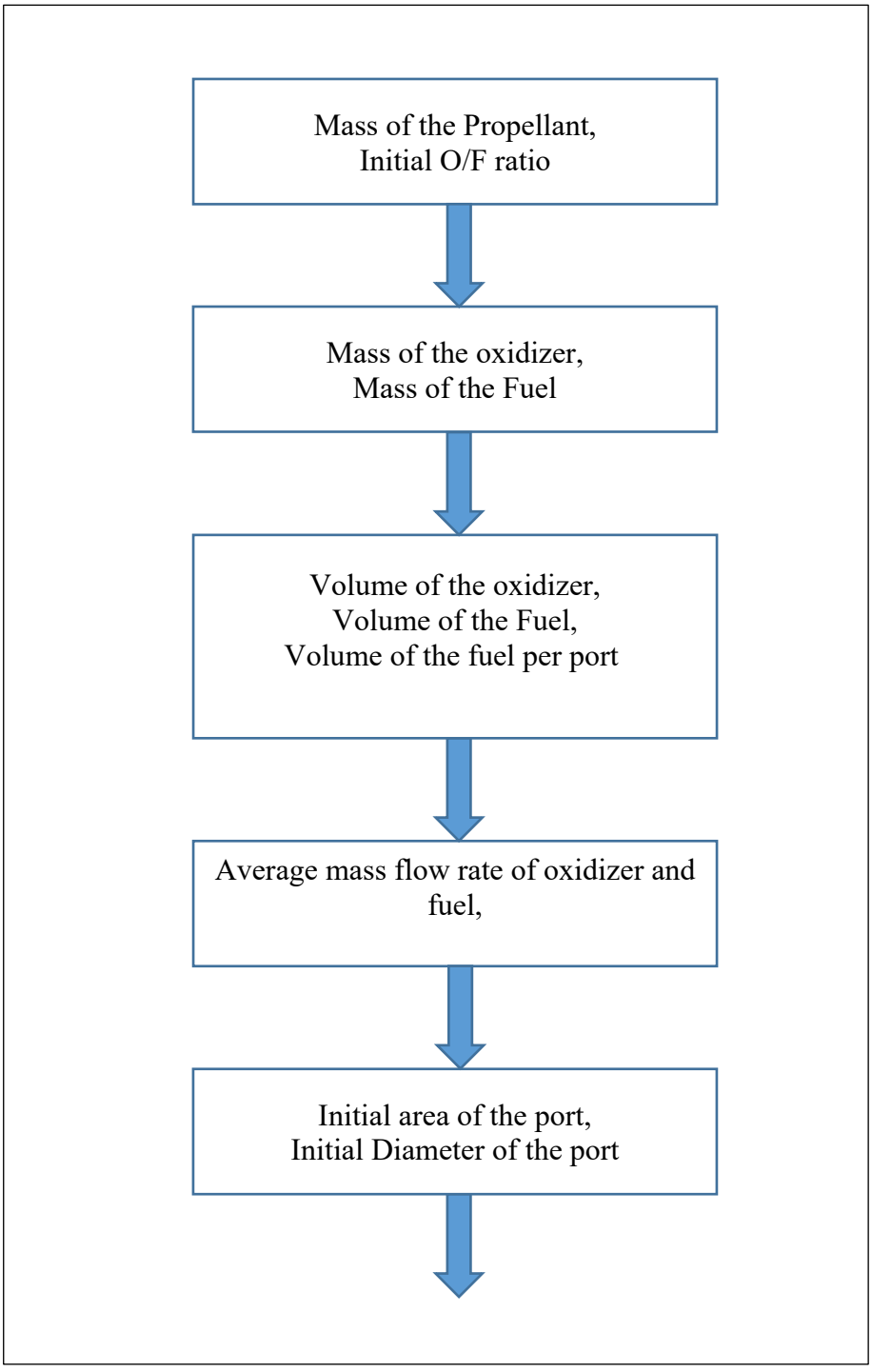

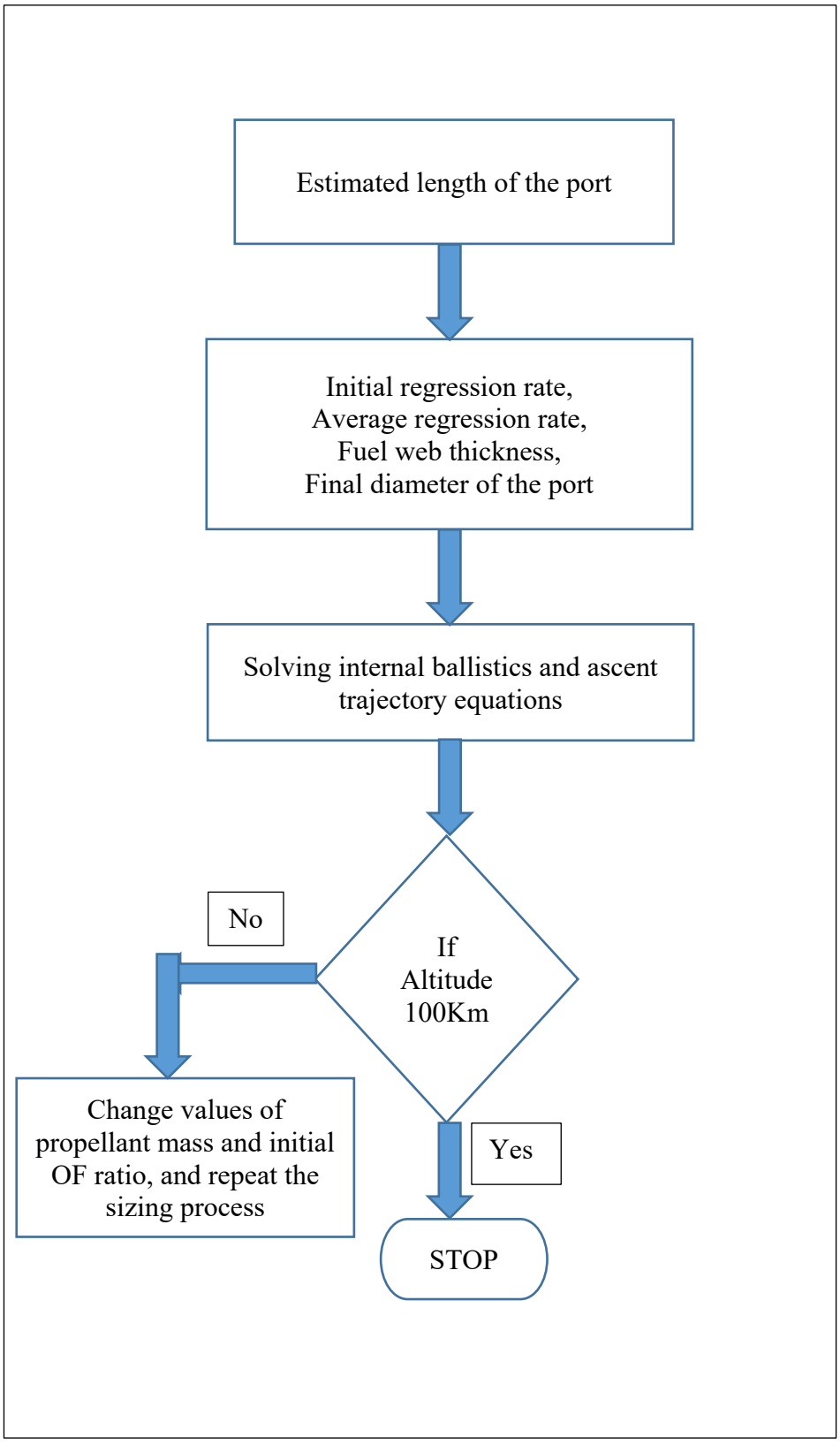
Estimated length of the port
Initial regression rate,
Average regression rate,
Fuel web thickness,
Final diameter of the port
Solving internal ballistics and ascent trajectory equations
If
Altitude
100Km
No
Change values of propellant mass and initial OF ratio, and repeat the sizing process
Yes
STOP

7.4.1. Constant Mass Flow Rate of the Oxidizer

The baseline case, where mass flow rate of the oxidizer is constant is considered as shown in Figure 6.1 to obtain the minimum propellant required to reach 100 Km altitude. The minimum amount of propellant is 1880 Kg. The best oxidizer to fuel ratio is 4.8.

Table 7.2

Optimal sizing for the case of a polynomial approximation of the control

M_p(initial)	O/F	Max Altitude	M_p(Used)
1900	3.12	79.03	1748.52
1900	4.85	105.6	1899.36
1870	4.8	99.73	1868.76
1880	4.8	101.5	1877.76

7.4.2. Polynomial Approximation

The mass flow rate of the oxidizer obtained from the genetic algorithm is approximated as a polynomial of degree 3 as shown in Figure 7.8. The minimum amount of propellant required to reach an altitude of 100 Km is 1840 Kg. The best oxidizer to fuel ratio is 2.8.

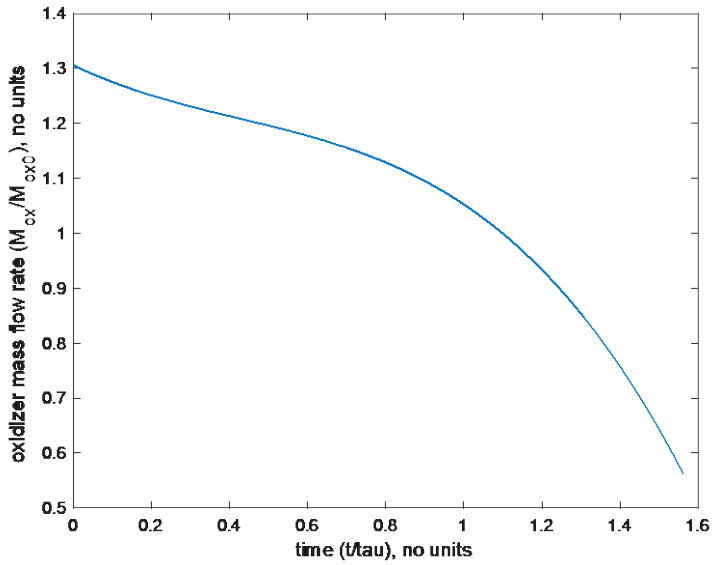

Figure 7.1 Polynomial approximation of optimal mass flow rate of the oxidizer obtained from genetic algorithm.

Table 7.3

Optimal sizing for the case of a polynomial approximation of the control

M_p(initial)	O/F	Max Altitude	M_p(Used)
1900	3.1	120.1	1942.56
1800	3	98.7	1835.64
1820	3	102.2	1854
1840	2.8	100	1839.6

7.4.3. Constant at the Maximum and then Linearly Decreasing

Next, we consider mass flow rate of the oxidizer similar to the solution obtained from genetic algorithm. In this case, the mass flow rate of the oxidizer is kept constant at the

maximum value, which is 30% higher the average oxidizer mass flow rate, until about one third of the burn time and then linearly decreased.

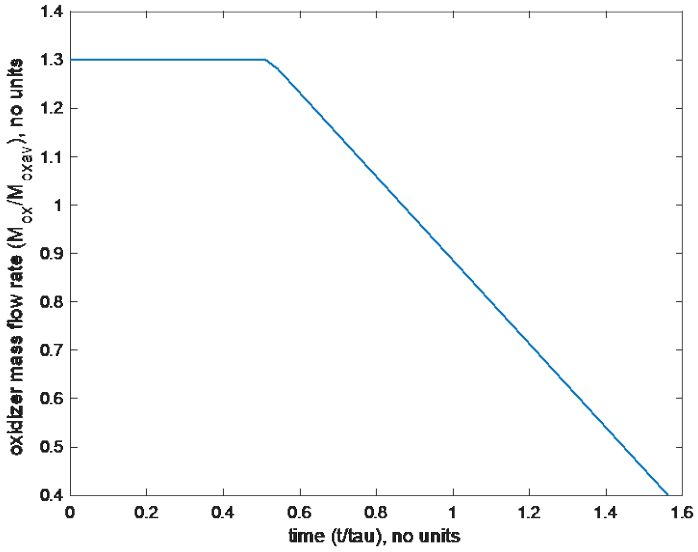

Figure 7.2 Constant mass flow rate of the oxidizer till one third of the burn time and then decrease linearly.

Table 7.1

Optimal sizing for the case of constant and then linearly decreasing control.

M_p(initial)	O/F	Max Altitude	M_p(Used)
1900	5	121.7	1919.88
1800	5	103.1	1827.36
1830	4.3	102.3	1820.44
1820	4.5	101	1815.12

7.4.4. Bang-Bang Control

Next, we consider bang-bang control in which the mass flow rate of the oxidizer is kept maximum till half of the burn time and then its minimum till the end of the burn. The maximum value of the oxidizer mass flow rate is 30% higher than the average mass flow rate of the oxidizer and the minimum value is 30% less than the average value.

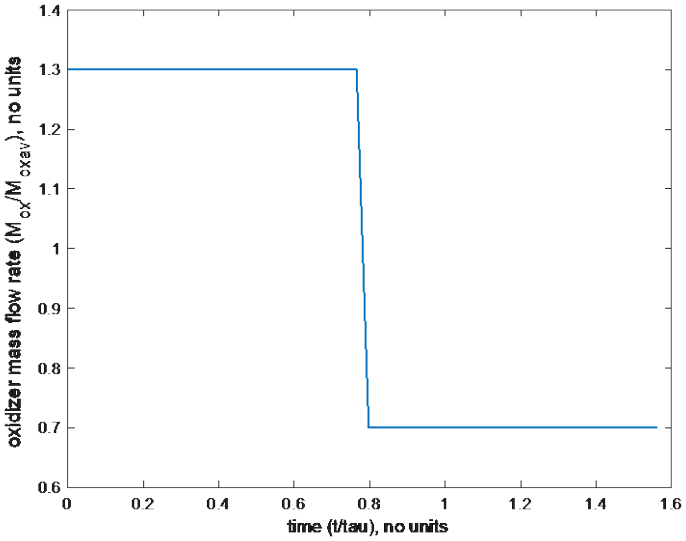

Figure 7.3 Bang-Bang control of oxidizer mass flow rate

Table 7.2

Optimal Sizing for Bang-Bang control

M_p(initial)	O/F	Max	M_p(Used)
1900	5	124.4	1920
1800	5	105.1	1848.96
1830	4.3	101.9	1828.08
1820	4.5	102.8	1836.72

From above four cases, the optimal solution is obtained to be constant mass flow rate of the oxidizer at maximum value until about one third of the burn time and then linearly decrease to a minimum value of mass flow rate of the oxidizer. The minimum propellant required to reach 100 Km altitude is 1820 Kg, and the initial OF ratio for is 4.5. The optimal size of the rocket can be obtained by considering these values for propellant mass and the initial OF ratio.

The initial diameter of the port D_{p0}, the final diameter of the port D_{pf}, the solid fuel web thickness w_f, and the length of the port L_P are obtained to be:

$$D_{p0} = 0.0984\ m; \qquad w_f = 0.0935\ \text{m};$$

$$D_{pf} = 0.2847\ m; \qquad L_P = 0.8878\ \text{m};$$

8. Effect of Regression Rate Law on Optimal Control

In this Chapter, we will discuss the internal ballistics of a hybrid rocket engine depending on the mass flux rate of the fuel and the mass flux rate of the oxidizer for seven circular ports, (Altman, 1991).

$$\dot{r}(t,x) = ax^m[G_f(t,x) + G_{ox}(t,x)]^n \tag{8.3}$$

As discussed in Chapter 3, by considering average regression rate along the port axis the regression rate equation can be written as:

$$\dot{r}(t,x) = ax^m[G_f(t) + G_{ox}(t)]^n \tag{8.2}$$

The oxidizer mass flux rate, fuel mass flux rate and the rate of change of hydraulic diameter are given by the following equations:

$$G_{ox}(t) = \frac{4\dot{m}_{ox}(t)}{\pi N D_H^2(t)} \tag{8.3}$$

$$G_f(t) = 4\rho_f a L_p^{m+1} \frac{1}{D_H(t)} \left[G_{ox}(t) + G_f(t)\right]^n \tag{8.4}$$

$$\frac{dD_H}{dt} = 2aL_p^m \left[\frac{4\dot{m}_{ox}}{\pi N D_H^2(t)} + G_f(t)\right]^n \tag{8.5}$$

To non-dimensionalize the internal ballistic equations, we substitute the non-dimensional parameters introduced in Chapter 3.

Substituting non-dimensional parameters in Equations (8.3), (8.4), and (8.5), we obtain flowing equations:

$$G_{ox}(t)\bar{G}_{ox}(\bar{t}) = \frac{4\dot{m}_{ox0}\bar{\dot{m}}_{ox}(\bar{t})}{\pi N D_{H0}^2 \bar{D}_H^2(\bar{t})} \tag{8.6}$$

$$G_{f0}\bar{G}_f(\bar{t}) = \frac{4\rho_f a L_p^{m+1}}{D_{H0}\bar{D}_H(\bar{t})}\left[\frac{4\dot{m}_{ox0}\bar{\dot{m}}_{ox}(\bar{t})}{\pi N D_{H0}^2 \bar{D}_H^2(\bar{t})} + G_{f0}\bar{G}_f(\bar{t})\right]^n \tag{8.7}$$

$$\frac{D_{H0}d\bar{D}_H}{\tau d\bar{t}} = 2aL_p^m\left[\frac{4\dot{m}_{ox0}\bar{\dot{m}}_{ox}(\bar{t})}{\pi N D_{H0}^2 \bar{D}_H^2(\bar{t})} + G_{f0}\bar{G}_f(\bar{t})\right]^n \tag{8.8}$$

By simplifying the above equations, we get the following equations in non-dimensional form:

$$\bar{G}_{ox}(\bar{t}) = \frac{\bar{\dot{m}}_{ox}(\bar{t})}{\bar{D}_H^2(\bar{t})} \tag{8.9}$$

$$\bar{G}_f(\bar{t}) = \left[\frac{(OF)_0}{(OF)_0+1}\right]^n \frac{1}{\bar{D}_H(\bar{t})}\left[\frac{\bar{\dot{m}}_{ox}(\bar{t})}{\bar{D}_H^2(\bar{t})} + \frac{\bar{G}_f(\bar{t})}{(OF)_0}\right]^n \tag{8.10}$$

$$\frac{d\bar{D}_H}{d\bar{t}} = 2\lambda_1\left[\frac{(OF)_0}{(OF)_0+1}\right]^n\left[\frac{\bar{\dot{m}}_{ox}(\bar{t})}{\bar{D}_H^2(\bar{t})} + \frac{\bar{G}_f(\bar{t})}{(OF)_0}\right]^n \tag{8.11}$$

The mass flow rate of the propellant in non-dimensional form can be written as:

$$\dot{m}_{p0}\bar{\dot{m}}_p(\bar{t}) = \dot{m}_{ox0}\bar{\dot{m}}_{ox}(\bar{t}) + \dot{m}_{f0}\bar{\dot{m}}_f(\bar{t}) \tag{8.12}$$

$$\bar{\dot{m}}_p(\bar{t}) = \left[\frac{(OF)_0}{(OF)_0+1}\right]\bar{\dot{m}}_{ox}(\bar{t}) + \left[\frac{1}{(OF)_0+1}\right]\bar{\dot{m}}_f(\bar{t}) \tag{8.13}$$

The fuel mass flow is given by:

$$\dot{m}_f(t) = \rho_f N\pi a L_p^{m+1} D_H(t)\left[G_f(t) + G_{ox}(t)\right]^n \tag{8.14}$$

The fuel mass flow rate in non-dimensional form is given by:

$$\bar{\dot{m}}_f(\bar{t}) = \left[\frac{(OF)_0}{(OF)_0+1}\right]^n \bar{D}_H(\bar{t})\left[\frac{\bar{\dot{m}}_{ox}(\bar{t})}{\bar{D}_H^2(\bar{t})} + \frac{\bar{G}_f(\bar{t})}{(OF)_0}\right]^n \tag{8.15}$$

We have the hydraulic diameter, the fuel mass flux rate, oxidizer mass flux rate, and the propellant mass flow rate in non-dimensional form. These equations are coupled non-linear differential equations. Unlike, the internal ballistic equations obtained in Chapter 3, in this case mass flux rate of the fuel cannot be obtained directly. To obtain the optimal control solution for mass flow rate of the oxidizer, we consider the dynamic equations to be hydraulic diameter equation and the ascent trajectory equations obtained in Chapter 5.

8.1. Optimal Control Solution

The optimal control obtained when regression rate is depending on mass flux rate of the oxidizer and the fuel behaves similar to the case where regression rate depends only on the mass flux rate of the oxidizer. The mass flow rate of the oxidizer is constant at maximum until about one third of burn time and then gradually decreased to the minimum value.

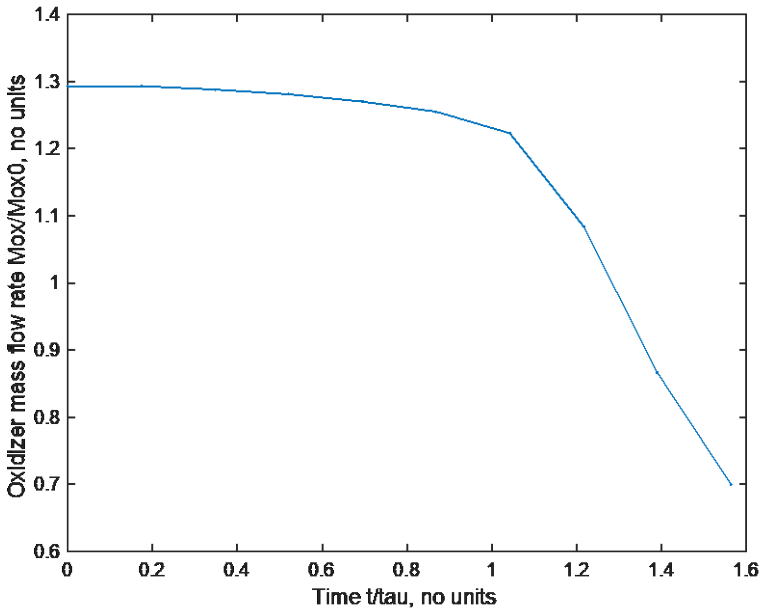

Figure 8.1 Optimal mass flow rate of the oxidizer obtained from genetic algorithm for regression rate depending on both oxidizer mass flux rate and the fuel mass flux rate.

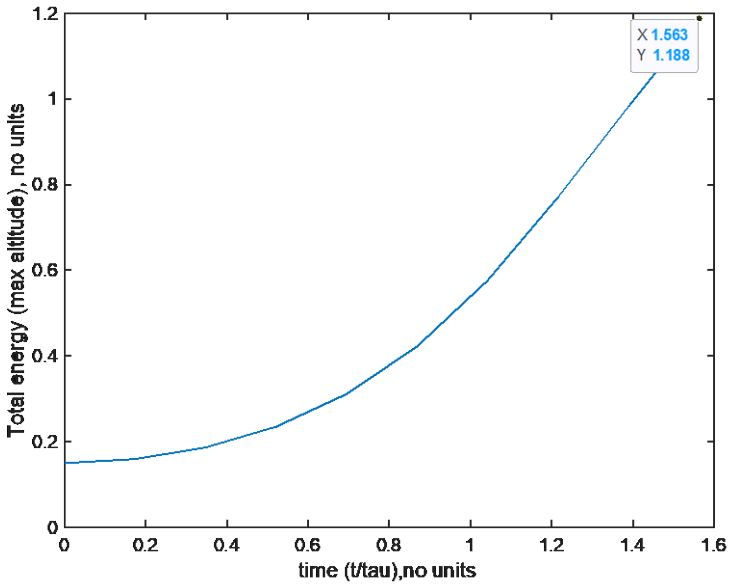

Figure 8.2 Total energy as a function of time for mass flow rate of the oxidizer obtained from genetic algorithm (total energy at burn time gives the maximum altitude reached).

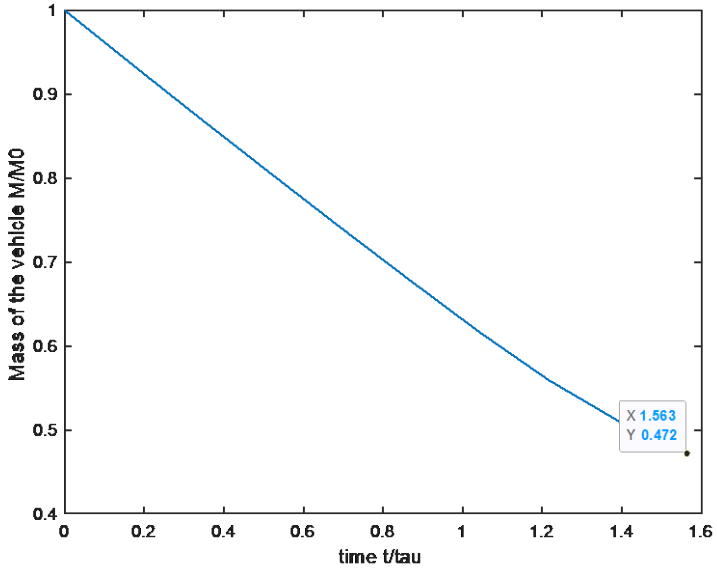

Figure 8.3 Mass of the vehicle as a function of time for optimal mass flow rate of the oxidizer.

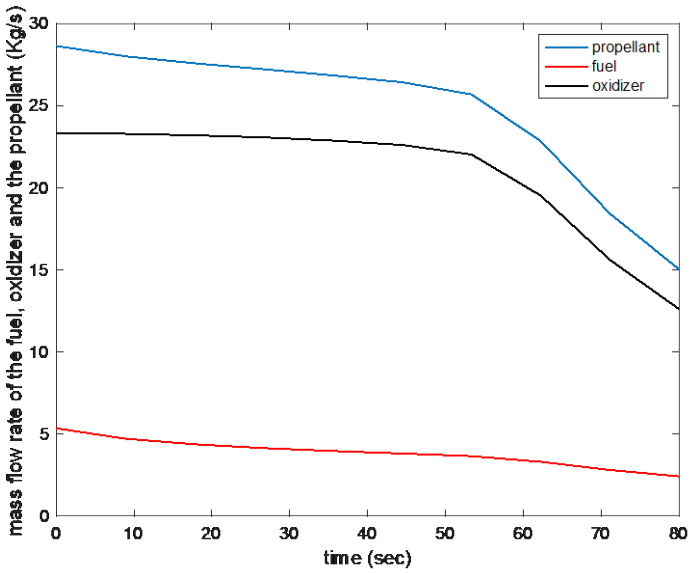

Figure 8.4. Mass flow rate of the oxidizer, the fuel, and the propellant obtained from genetic algorithm when regression rate is depending on mass flux rate of the oxidizer and the fuel.

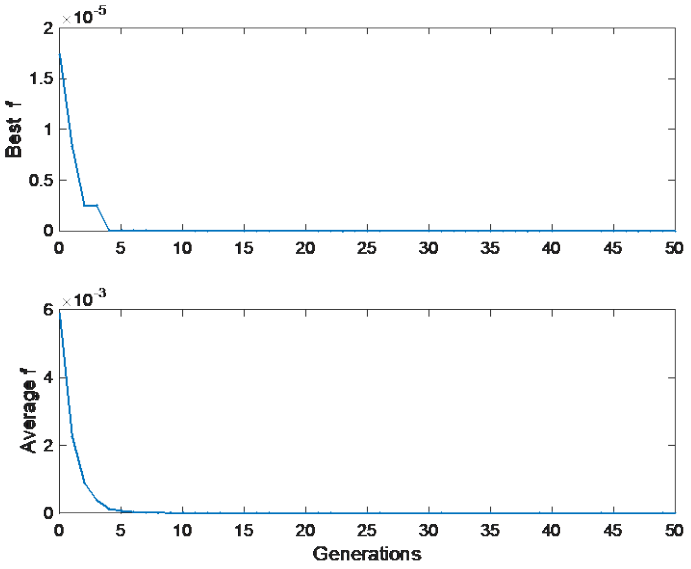

Figure 8.5 Genetic algorithm convergence of fitness function.

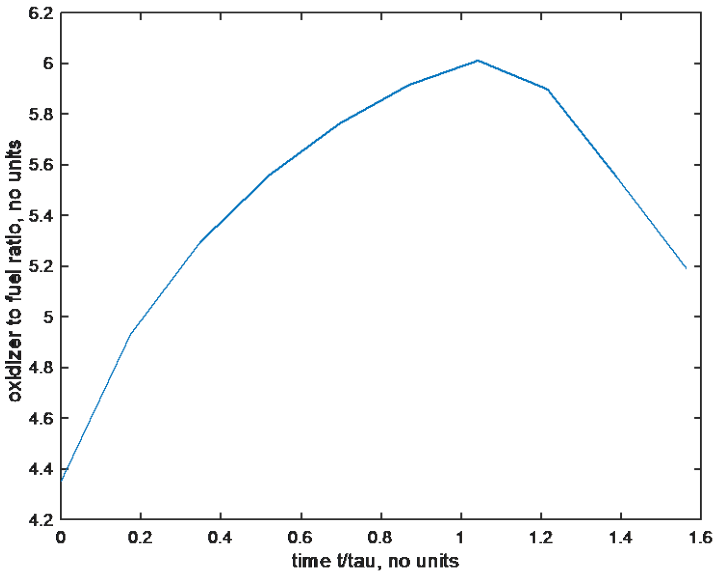

Figure 8.6 Oxidizer to fuel ratio for optimal mass flow rate of the oxidizer.

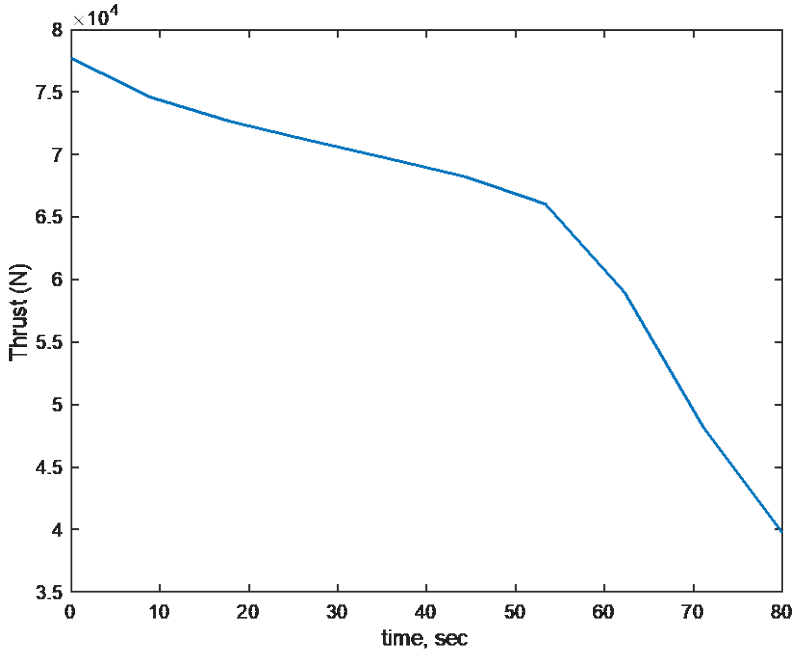

Figure 8.7 Thrust as a function of time for optimal mass flow rate of the oxidizer.

9. Conclusions

We are considering the performance of a hybrid rocket vehicle in a sub-orbital mission such as space tourism. First, we study the effect of throttling by considering three different mass flow rates of the oxidizer as a function of time. We considered a constant mass flow rate of the oxidizer, linearly increasing and linearly decreasing such that the amount of oxidizer is same in all the cases. From the results, it is observed that the performance of a rocket can be enhanced by controlling the mass flow rate of the oxidizer, and the altitude reached for linearly decreasing mass flow rate of the oxidizer case was maximum.

Next, the optimal mass flow rate of the oxidizer was obtained as a function of time using a genetic algorithm in order to maximize the altitude reached for a fixed amount of propellant. The optimal solution for the mass flow rate of the oxidizer as a function of time is obtained to be constant at the maximum for about one third of the burn time and then gradually decreases. Next, we consider the problem of optimal sizing of the vehicle using the solution obtained from the genetic algorithm. The minimum propellant required to reach 100 Km altitude and the optimal initial OF ratio are obtained. The minimum propellant required is 80 Kg less than the base line case, for which the amount of propellant given is 1900 Kg.

This work can be extended to solve more realistic models of internal ballistics by considering the variation of the burn along the axial direction. In this problem, a one-dimensional trajectory was considered. This method can be applied to optimize two-dimensional trajectories. The necessary conditions provided by the Pontryagin's maximum principle were not solved. Those equations can also be solved to check for the optimality.

REFERENCES

Altman, D. (1991). Hybrid rocket development history. In 27th *AIAA Joint Propulsion Conference, Sacramento-CA, 2515*. doi: 10.2514/6.1991-2515.

Ben-Asher, J. Z. (2010). *Optimal control theory with aerospace applications*. America Institute of Aeronautics and Astronautics, Reston, Virginia. doi: 10.2514/5.9781600867347.0001.0007

Betts, J. (2001). *Practical Methods for Optimal Control Using Nonlinear Programming. SIAM, Society for Industrial and Applied Mathematics, Philadelphia, PA*.

Berkovitz, L. D. (1961). Variational methods in problems of control and programming. *Journal of Mathematical Analysis and Applications*, *3*(1), 145–169. doi: 10.1016/0022-247X(61)90013-0

Breakwell, J. V., Speyer, J. L., & Bryson, A. E. (1963). Optimization and Control of Nonlinear Systems Using the Second Variation. *Journal of the Society for Industrial and Applied Mathematics. Series A, On Control*, *1*(2), 193–223. doi: 10.1137/0301011

Breakwell, J. V., & Yu-Chi, H. (1965). On the conjugate point condition for the control problem. *International Journal of Engineering Science*, *2*(6), 565-579. doi: 10.1016/0020-7225(65)90037-6

Bushaw, D. W. (1953). Differential equations with a discontinuous forcing term, Stevens Inst of Tech Hoboken NJ Experimental Towing Tank, January 01, New Jersey.

Bushaw, D. (1958). "Optimal discontinuous forcing terms," Contributions to the theory Of nonlinear oscillations, 4, 29-52. doi: 10.1515/9781400881758-004

Cai, G., Zhu, H., Rao, D., & Tian, H. (2013). Optimal design of hybrid rocket motor powered vehicle for suborbital flight. *Aerospace Science and Technology*, *25*(1), 114–124. doi: 10.1016/j.ast.2011.12.014

Casalino, L., & Pastrone, D. (2005). Oxidizer Control and Optimal Design of Hybrid Rockets for Small Satellites. *Journal of Propulsion and Power*, *21*(2), 230–238. doi: 10.2514/1.6556

Casalino, L., & Pastrone, D. (2010). Optimal Design of Hybrid Rocket Motors for Launchers Upper Stages. *Journal of Propulsion and Power*, *26*(3), 421–427. doi: 10.2514/1.41856

Casalino, L., & Pastrone, D. (2012). Optimization of Hybrid Sounding Rockets for Hypersonic Testing. *Journal of Propulsion and Power*, *28*(2), 405–411. doi: 10.2514/1.B34218

Casalino, L., Pastrone, D., & Simeoni, F. (2015). Approximate and Exact Approaches for the Optimization of Hybrid-Rocket Upper Stage. *Journal of Propulsion and Power*, *31*(2), 765–769. doi: 10.2514/1.B35462

Casalino, L., Masseni, F., & Pastrone, D. (2018). "Optimization of Hybrid Rocket Engines for Small Satellite Launchers." *Joint Propulsion Conference* (p. 4926), July 8, Cincinnati, Ohio. doi:10.2514/6.2018-4926

Chiaverini, M. J. (2000). *Fundamentals of hybrid rocket combustion and propulsion*. American Institute of Aeronautics and Astronautics, Reston, Virginia.

Coleman, T. F., & Liao, A. (1995). An efficient trust region method for unconstrained discrete-time optimal control problems. *Computational Optimization and Applications*, *4*(1), 47–66. doi: 10.1007/BF01299158

Crispin, Y. (2007). Evolutionary Computation for Discrete and Continuous Time Optimal Control Problems. In *Informatics in Control, Automation and Robotics II* (pp. 59–69). Springer Netherlands. doi: 10.1007/978-1-4020-5626-0_8

Fox, C. (1987). *An introduction to the calculus of variations*. Dover Publication: New York.

Hestenes, M. R. (1950). A general problem in the calculus of variations with applications to paths of least time. Rand Corp Santa Monica, CA.

Kelley, H. (1962). Guidance theory and extremal fields. *I.R.E. Transactions on Automatic Control*, *7*(5), 75–82. doi: 10.1109/TAC.1962.1105503

Kelley, H. J., Kopp, R. E., & Moyer, H. G. (1967). Singular extremals, Topics in Optimization, G. Leitmann, ed., New York. doi: 10.1016/S0076-5392(09)60039-4

Kelley, H. J. (1973). Aircraft maneuver optimization by reduced-order approximation. In Control and Dynamic Systems (Vol. 10, pp. 131-178). Academic Press. doi:10.1016/B978-0-12-0127-0-8.50009-1

Kim, Y. H., & Spencer, D. B. (2002). Optimal Spacecraft Rendezvous Using Genetic Algorithms. *Journal of Spacecraft and Rockets*, *39*(6), 859–865. doi: 10.2514/2.3908

Larson, W. J., Henry, G. N., & Humble, R. W. (Eds.). (1995). *Space propulsion analysis and design*. McGraw-Hill.

Liao, L.-Z., & Shoemaker, C. (1991). Convergence in unconstrained discrete time differential dynamic programming. *IEEE Transactions on Automatic Control*, *36*(6), 692–706. doi: 10.1109/9.86943

Lippisch, A. (1946). "Performance theory of airplanes with jet propulsion." Headquarters Air Materiel Command, Translation Report no. F-TS-685-RE, New York. doi: 10.2514/8.1314

Mayne, D. (1996). "A second-order gradient method for determining optimal trajectories of non-linear discrete-time systems." International Journal of Control, 3(1), 85-95.

Michalewicz, Z.,(1996). *Genetic algorithms+ data structures= Evolution programs.* Springer Science & Business Media, Springer- Verlag, Berlin.

Murray, D. M., & Yakowitz, S. J. (1984). Differential dynamic programming and Newton's method for discrete optimal control problems. *Journal of Optimization Theory and Applications*, *43*(3), 395–414. doi: 10.1007/BF00934463

Park, C., Guibout, V., & Scheeres, D. J. (2006). Solving Optimal Continuous Thrust Rendezvous Problems with Generating Functions. *Journal of Guidance, Control, and Dynamics*, *29*(2), 321–331. doi: 10.2514/1.14580

Pontr͡iagin, L. S. (1987). *Mathematical theory of optimal processes*. Gordon and Breach Science Publishers, New York. doi: 10.1201/9780203749319

Rao, D., Cai, G., Zhu, H., & Tian, H. (2012). Design and optimization of variable thrust hybrid rocket motors for sounding rockets. *Science China. Technological Sciences*, *55*(1), 125–135. doi: 10.1007/s11431-011-4597-4

Rhee, I., Lee, C., & Lee, J.-W. (2008). Optimal design for hybrid rocket engine for air launch vehicle. *Journal of Mechanical Science and Technology*, *22*(8), 1576–1585. doi: 10.1007/s12206-008-0514-6

Ross, I. M. (2015). "A primer on Pontryagin's principle in optimal control." Collegiate publishers, San Francisco.

Schoonover, P. L., Crossley, W. A., & Heister, S. D. (2000). Application of a Genetic Algorithm to the Optimization of Hybrid Rockets. *Journal of Spacecraft and Rockets*, *37*(5), 622–629. doi: 10.2514/2.3610

Van Laarhoven, P. J., & Aarts, E. H. (1987). "Simulated annealing. In Simulated annealing: Theory and applications." (pp. 7-15), Springer, Dordrecht.

Vinter, R. (2002). Dynamic optimization Arthur E. Bryson; Addison-Wesley Longman, Inc., Reading, MA, 1999. *Automatica (Journal of IFAC)*, *38*(10), 1831-1833. doi: 10.1016/S0005-1098(02)00084-5.

Vonderwell, D. J., Murray, I. F., & Heister, S. D. (1995). Optimization of hybrid-rocket-booster fuel-grain design. *Journal of Spacecraft and Rockets*, *32*(6), 964–969. doi: 10.2514/3.26716

Publications

Ryakam, S., “Effect of Ascent Trajectory on Hybrid Rocket Sizing,” Master’s Thesis, Embry-Riddle Aeronautical University, 2017.

Ryakam, Srija, and Yechiel, Crispin. "Optimal Control of Hybrid Rocket for Sub-orbital Ascent Trajectory." *AIAA Propulsion and Energy 2021 Forum*. 2021.